1990

Strain and Volume Loss in a Second Order Buckle Fold, Central Appalachian Valley and Ridge, U.S.A.

Michelle J. Markley
Oberlin College

Strain and Volume Loss in a Second Order Buckle Fold, Central Appalachian Valley and Ridge, U.S.A.

Michelle Markley
May 3, 1990

Introduction

Large scale thrusts and imbricates overlain by folded sedimentary strata characterize structure in the Valley and Ridge Province of the Central Appalachians (Woodward, 1989; Meyer and Dunne, 1990). The Cambrian Waynesboro Formation is a decollement zone that detached an imbricated Cambro-Ordovician sequence from an unfaulted Pre-Cambrian basement (Woodward, 1989). The Ordovician Martinsburg Shale is a second zone of major detachment that de-coupled the blind thrust system in the Cambro-Ordovician carbonates from the overlying orogenic wedge (Woodward, 1989). Thus, the Central Valley and Ridge deformed during the late Paleozoic Alleghenian orogeny as a three tiered system consisting of the undeformed basement, the imbricated stiff layer, and the primarily folded cover layer (Perry, 1978; figures 1 and 2).

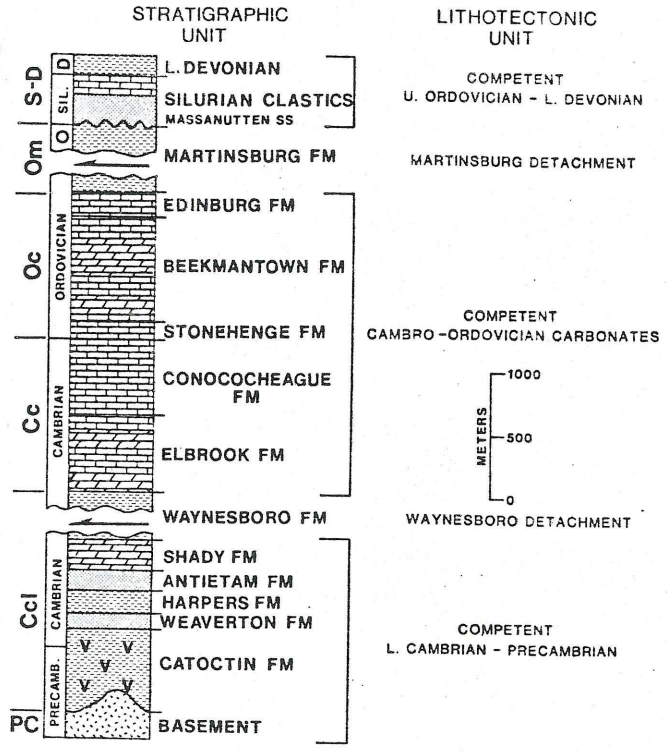

Figure 1: Stratigraphic column for Central Valley and Ridge (from Woodward, 1989).

Figure 2: Regional map, stratigraphic column for cover strata, and regional cross sections of the Valley and Ridge (from Woodward, 1989). The dark arrow points to the fold on Martin Mountain.

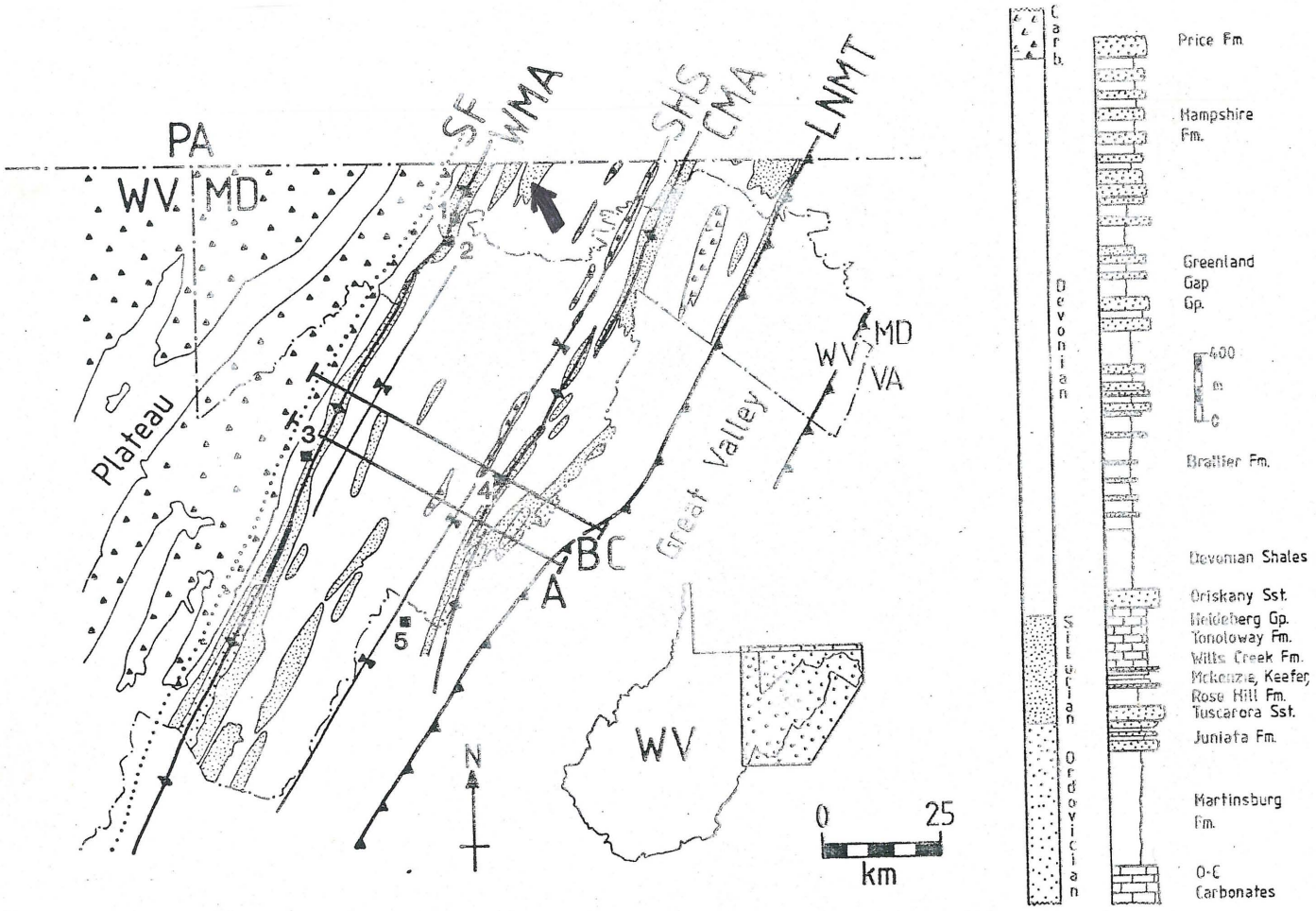

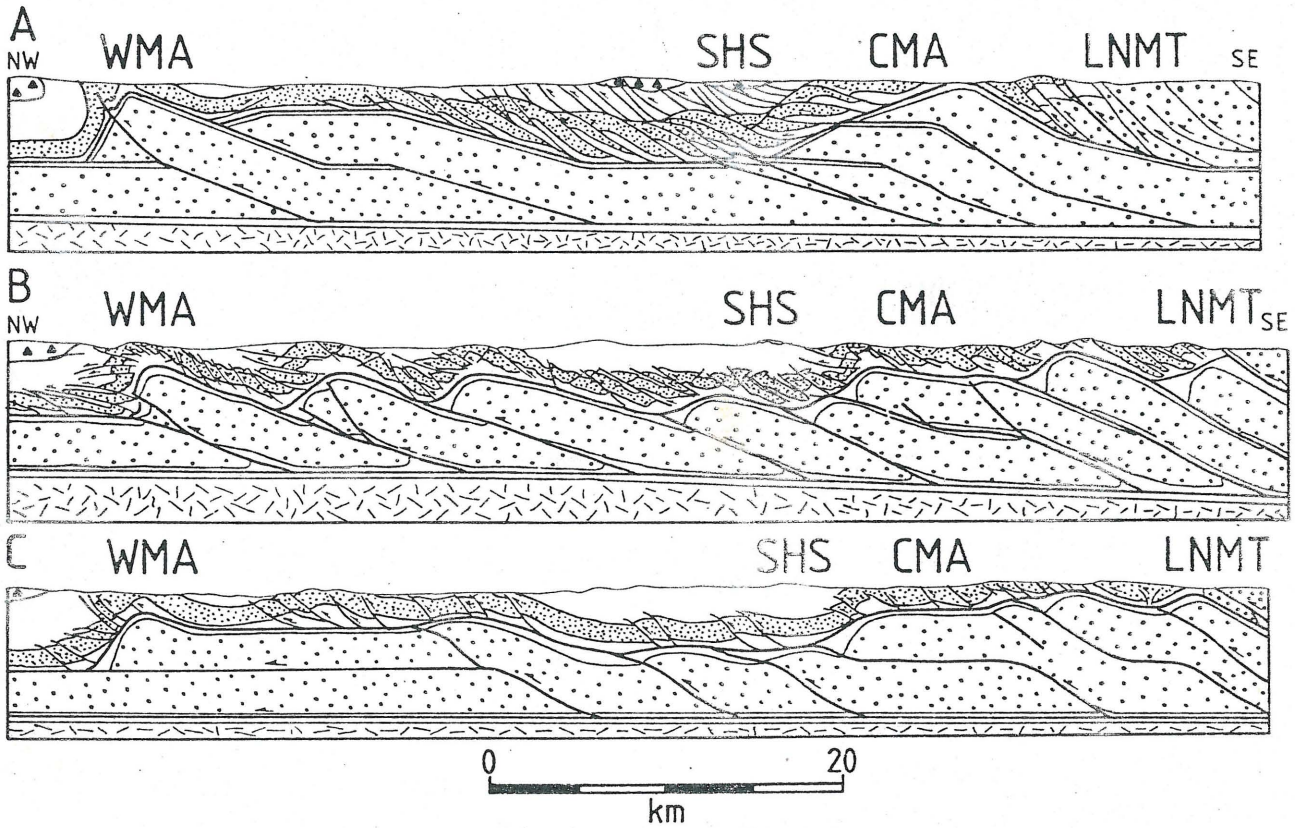

A road cut along the eastern side of Martin Mountain exposes a smaller (probably second-order) fold in the Silurian Tonoloway limestone that belongs to the cover layer (figures 3 and 4). This anticline is one of a train of regular folds with wavelengths of 150 to 250 m. (DeWitt and Colton, 1964). A small hinge region and symmetrical planar limbs characterize this angular, open anticline. Bed thickness remains relatively constant throughout the fold, making it a class IB (parallel) or IC fold. The anticlinal hinge trends 28° east of north and dips 8° to the north. A poorly exposed, smaller syncline flanks its eastern limb.

The Tonoloway Limestone formed during the late Silurian on a carbonate platform (Woodward, 1989). During Paleozoic deformation, it lay under 3 km of sediments (Meyer and Dunne, 1990) at a temperature of 250°C (Mitra, 1987). This outcrop exposes only 80 m of the 550 m thick formation (DeWitt and Colton, 1964). Cathodoluminescence reveals that the sediments comprise only calcite, dolomite, organic rich clays, and trace amounts of quartz. These fine-grained arenites and lutites display neither noteworthy fossil content nor sedimentary structures oblique to bedding. Bed thicknesses vary from 0.5 m. to 2 m.; planar lamination defined by grain size and clay content occurs in most beds.

Slickensides on primary bedding surfaces indicate that flexural slip was an important mechanism during folding (Ramsay, 1967). Mesoscopic and microscopic structures accommodate strain within the layers. Two morphologically distinct cleavages within the fold are non-coaxial. Clay selvage seams indicate that both cleavages resulted from pressure solution. Whereas one spaced

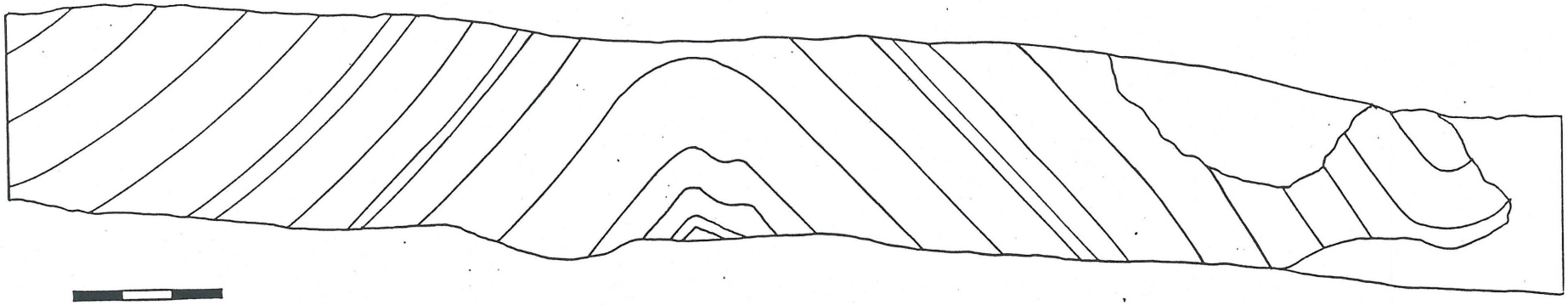

Figure 3: hypothetical cross section of the fold constructed parallel to the profile plane. The scale bar is 15 m long.

Figure 4: The fold hinge region in outcrop exposure.

cleavage fans convergently around the fold hinge in the more competent beds, the second, more penetrative cleavage fans divergently around the fold hinge in the less competent beds. The non-coaxiality of these two cleavages helps define the chronology of and tectonic stress field during the shortening event that produced the cleavages and the fold (Gray, 1981).

In addition to establishing a deformation history of folding, mesoscopic and microscopic structures speak to the question of strain behavior and layer rheology of the folded Tonoloway Limestone. The persistence of pressure solution surfaces and fibrous veins throughout the fold suggest linear or Newtonian behavior in the deformed strata (Elliott, 1973). In the fold limbs, twinning and undulose extinction patterns in calcite crystals signal power law or plastic behavior (Mitra, 1978). Fold geometry, layer rheology, and geologic setting suggest that buckling best defines the mechanism of folding here (Hudleston,1973).

In the Central Valley and Ridge, new cross sections show that the stiff tier of thrusts and imbricates controls megascopic structural morphologies in the cover layer (Woodward, 1985). Regional anticlinoria and synclinoria formed by either fault bend folding (Suppe, 1983) or passive kinking (Faill, 1973) during emplacement of imbricates in the stiff layer. The train of second order buckles, in which this exposed anticline formed, occurs, however, in a smaller scale environment, which, although it allowed for local buckling, results from the geometry of regional imbrication in the stiff layer (Suppe, 1983; Dunne, 1989).

Traditionally, cross sections of this region fail to provide a long enough cover layer to blanket the unthrusted stiff layer (Geiser, 1988). Volume loss strain (i.e. loss through percolating meteoric fluids) in shallow deformed rocks may account for one element of this problem with balancing the two tiers together (Geiser, 1988). If volume loss strain is more significant in one layer than in the other, an unraveled cross section naturally displays an unbalance between the two. Although volume loss strain directly relates to structures and strain patterns, this phenomenon has interested geologists only recently (cf. Bell and Cuff, 1989). As a result, no general methodology exists for measuring it. Volume loss strain challenges the notion that structures such as folds and cleavages develop within a closed system, in which material dissolved in areas of high stress reprecipitates locally in areas of low stress (Weyl, 1959). Volume loss strain, however, requires an open system from which foreign fluids introduced by significant dewatering or infiltration remove material (Engelder, 1984).

Mesoscopic and Microscopic Structures

Introduction

In the Martin Mountain fold, limb-dips range from 0° at the hinge to 50° on the outer-limb exposures. Because of the angularity of the hinge and the straight limbs, however, limb-dips of 0° to 30° describe the hinge region. Structures present at a limb-dip of 40° are midway between the hinge and the farthest limb exposure. Stereographic projections of poles to bedding surfaces in a typical rounded fold cluster in a great circle, the Π circle (Marshak and Mitra, 1988; figure 5). The pole to the Π circle defines the fold hinge axis. Even if they are oblique to bedding, structures within the fold that trend parallel to the fold axis define a great circle parallel to the Π circle. The Π circle also defines the orientation in space of the profile plane of the fold, a surface normal to the hinge axis that provides the most accurate cross-section. In this fold, the Π circle defines a fold axis at 028,08 (figure 6).

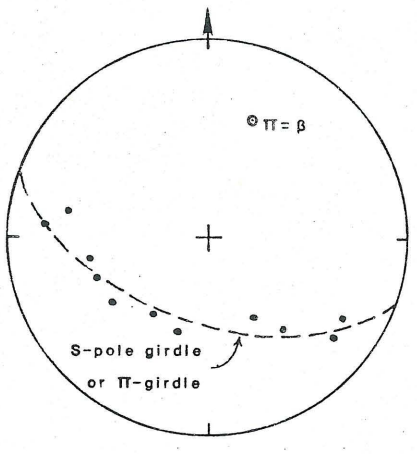

Figure 5: Poles to bedding surfaces in a typical rounded fold. the Π circle parallels the profile plane. Π (or ß) parallels the hinge axis.

Figure 6: Poles to bedding.

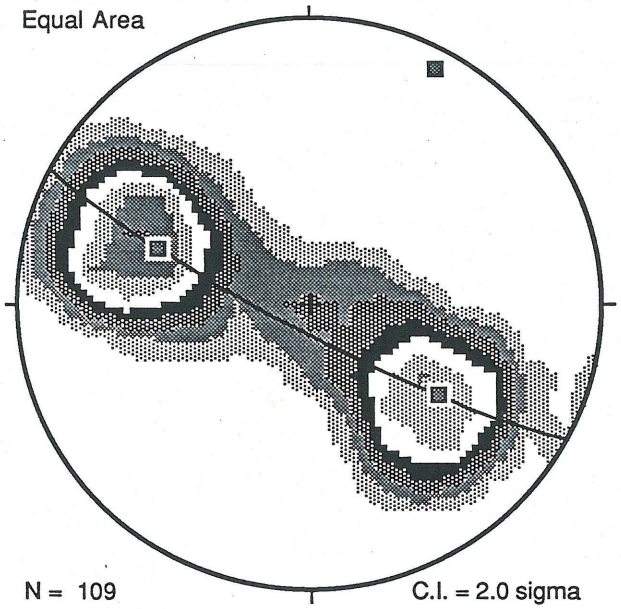

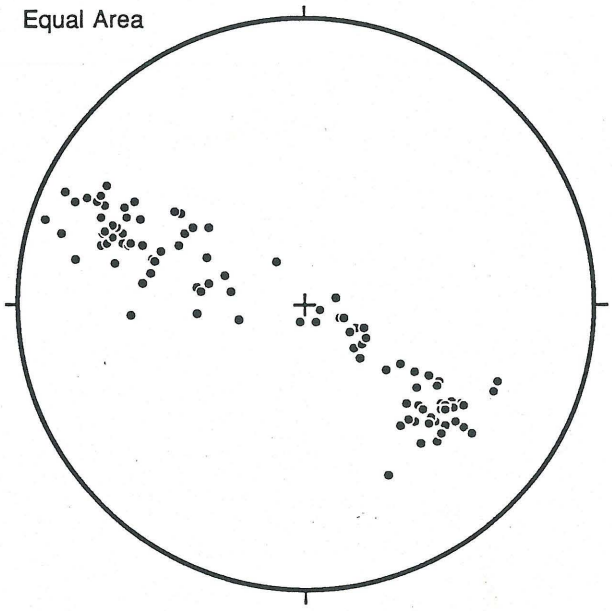

poles to bedding

poles to bedding
pole to great circle 028,08
trend and plunge of fold axis 028,8

Figure 7: Kinematic rotation axes.

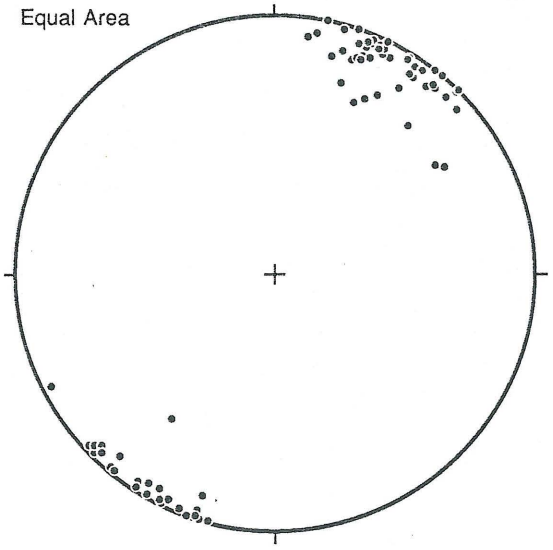

kinematic rotation axes

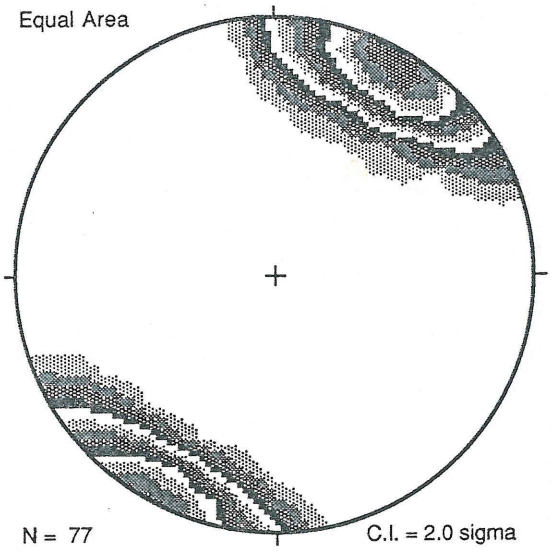

kinematic rotation axes
point maximum 029,07

Bed-parallel slip surfaces

Calcite-fiber slickensides on primary bedding surfaces indicate bedding-parallel slip. Most bed-parallel slip surfaces persist for several meters parallel to dip, suggesting that slip concentrated along individual bedding planes rather than stepping from one surface to another . In detail, 1 to 10 mm thick packets of untwinned calcite fibers compose the slickensides. The long axes of calcite fibers in the slickensides typically parallel primary bedding, but blocky, randomly-oriented calcite crystals replace fibers in the central portions of some slickensides. The long axes of the calcite fibers point down the dip of bedding. Slickenside geometry is consistent with an origin due to bed-parallel slip during flexural folding (Ramsay and Huber, 1987). Bed-parallel slip surfaces used pre-existing discontinuous bedding surfaces, which are spaced 0.5 to 2 m apart.

Kinematic rotation axes for bed parallel slip surfaces define a point maximum at 029,07 (figure 7), almost exactly parallel to the hinge axis defined by the Π circle. Slip occurred symmetrically around the hinge, and slickensides consistently show a top towards the hinge offset.

Interbed Cleavage

Two morphologically distinct spaced cleavages cut beds in this fold (figure 8). Here, as in most folds (Gray, 1981), spaced cleavage formed by pressure solution. One type, interbed cleavage, has the stylolitic habit typical of widely spaced, incipient pressure solution (Alvarez et al., 1978; figure 9). Interbed cleavage occurs within

Figure 8: Two morphologically distinct spaced cleavages.

Figure 9: Stylolitic interbed cleavage.

individual beds, but often continues into neighboring beds. Surfaces have well developed teeth in arenites, but are relatively planar in lutites. Within a given bed, interbed cleavage surfaces are evenly spaced; as grain size decreases or as clay content increases, spacing ranges from 0.5 m to 10 cm. Interbed cleavage, best preserved in more resistant beds, is within 5° of normal to bedding, forming the pattern of a convergent cleavage fan. It exhibits a consistent morphology throughout the anticline, although it intensifies in the hinge region. Shortening across interbed cleavage surfaces, calculated from bedding offsets or dissolved fossils, shows that individual seams record losses of 5 mm to 5 cm of material measured normal to the seam. The more closely spaced seams record less loss than the well spaced seams. Thus, interbed cleavage accounts for approximately 10% shortening normal to bedding.

In thin section, interbed cleavage seams are thick collections of clay selvage. The selvage has no distinct clay-like platy structure, and cathodoluminescence studies suggest that the selvage contains more organic material than clay. Thus, concentration along pressure solution seams involved concentration but not rotation of the organic material.

Notably, other mesoscopic structures, such as faults, small folds, and veins, crosscut interbed cleavage. Bed parallel faults occasionally offset interbed cleavage in one bed from its continuation in a neighboring bed. In arenites and dolomites, extensional veins at obtuse angles to bedding either cut across or fill interbed cleavage seams. In lutites, intrabed cleavage cuts and

often completely obscures interbed cleavage. Interbed cleavage formed early relative to other structures. In competent arenitic and dolomitic beds, interbed cleavage survives in the midst of later deformational structures. In these beds, interbed cleavage probably remained active throughout folding, but the less competent beds exhibit other strain paths.

A stereographic projection of poles to interbed cleavage supports the argument for early formation. If interbed cleavage formed during folding, poles to cleavage would define a great circle parallel to the Π circle (Helmstaedt and Greggs, 1980). Instead, the great circle defines a pole at 041,06 (figure 10). This trend diverges a full

Figure 10: Poles to interbed cleavage.

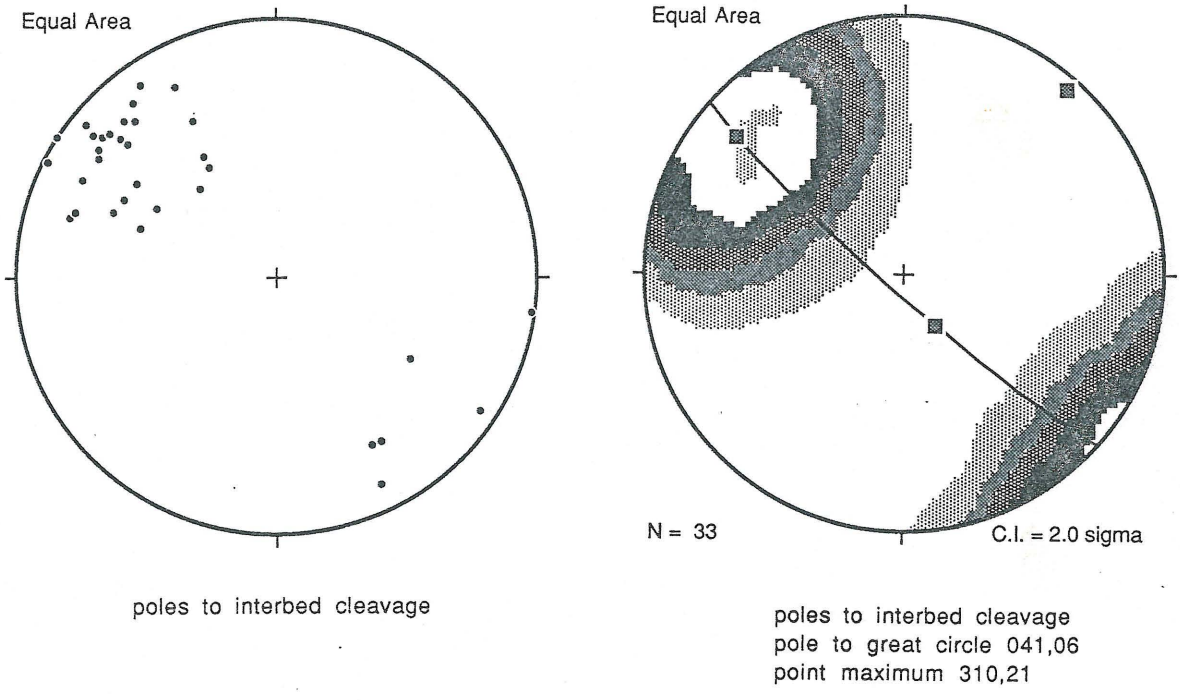

poles to interbed cleavage

poles to interbed cleavage
pole to great circle 041,06
point maximum 310,21

13° from the fold axis inferred from both bedding and kinematic rotation axes. In addition to this, poles to the other spaced cleavage, intrabed cleavage, define a great circle parallel to the Π circle. In a sample cut parallel to bedding, interbed cleavage and intrabed cleavage diverge by 15°. Thus, while slickensides and intrabed cleavage show orientations conformable with the fold hinge, interbed cleavage, although it fans around the fold hinge, does not parallel the hinge.

Evidence from stereographic projections and crosscutting relationships indicates that the formation of interbed cleavage not only predates structures formed in late stages of folding, it may predate folding itself. In general, interbed cleavage remained bed normal throughout folding, rotating passively with bedding around the fold hinge. Early interbed cleavage surfaces remained active as sites of strain only in the more competent beds.

Intrabed Cleavage

A morphologically distinct cleavage, intrabed cleavage, occurs as closely spaced parallel seams consistently inclined to bedding (figure 11). Although intrabed cleavage often occurs in neighboring beds, individual seams never cross bedding discontinuities. Because of its inclined angle to bedding, intrabed cleavage fans divergently around the fold hinge. Although intrabed cleavage occurs in the limbs of the fold, it is most intense at limb-dips of 0° to 40°. Intrabed cleavage is also better developed in fine-grained and clay rich beds than interbed cleavage. Intrabed cleavage is more visible in outcrop than interbed cleavage; it is often penetrative in thin

Figure 11: Intrabed cleavage and en echelon vein arrays.

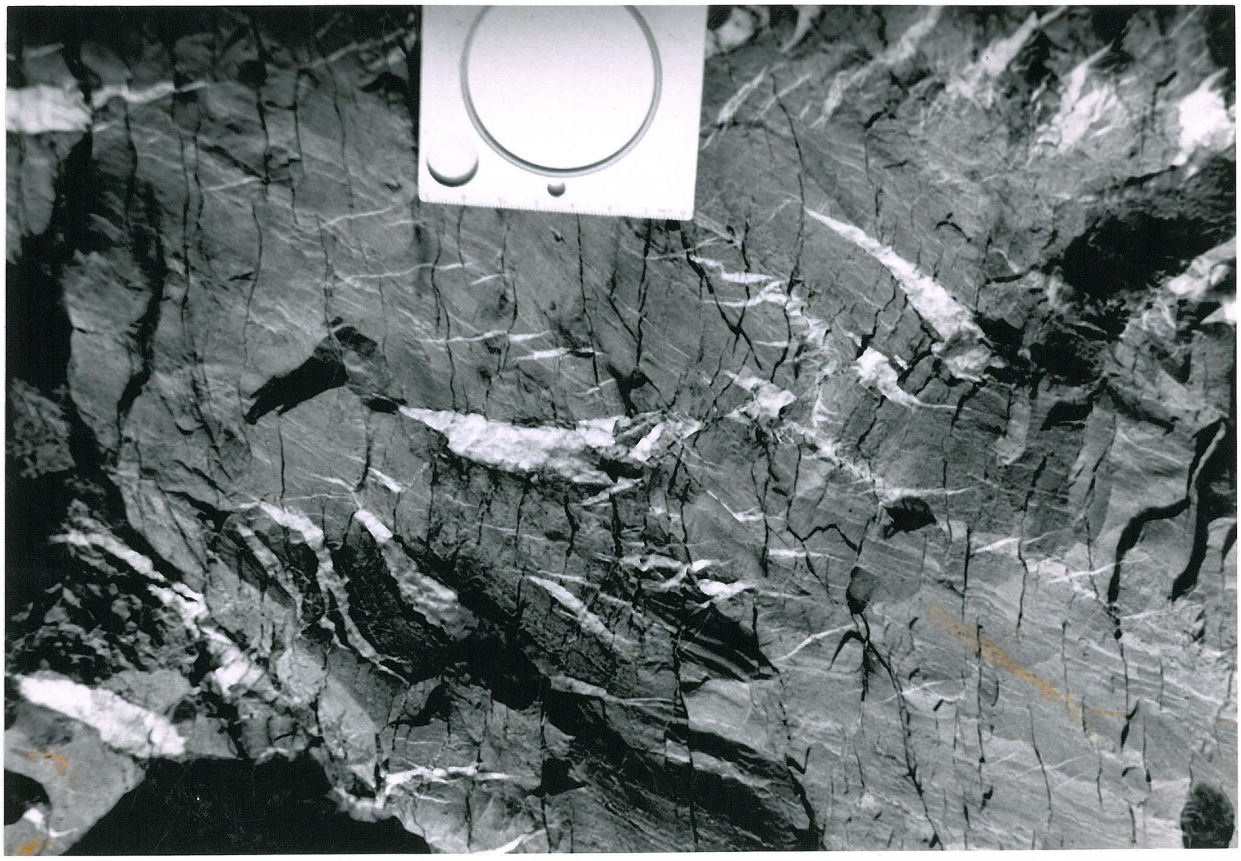

Figure 12: Poles to intrabed cleavage.

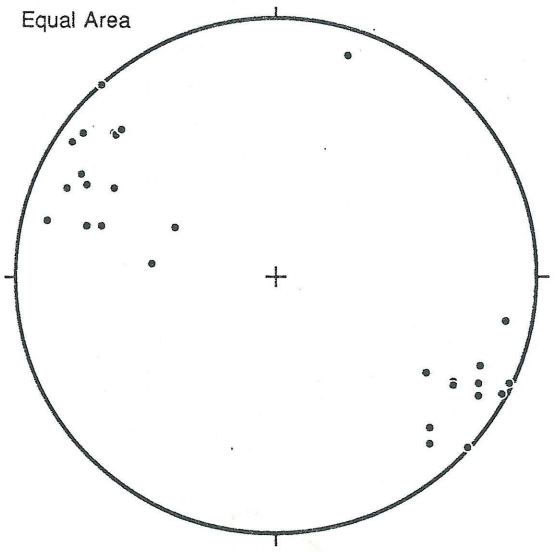

poles to intrabed cleavage

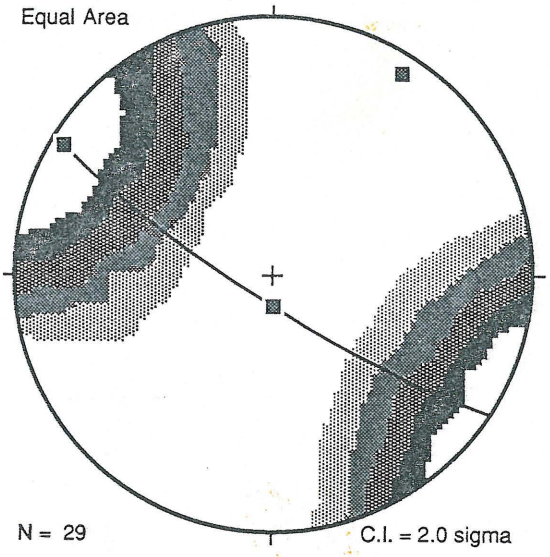

poles to intrabed cleavage
pole to great circle 033,08
point maximum 302 05

section. On all scales, intrabed cleavage shows orientations and a geometric relationship with bedding that indicate an origin due to shearing parallel to bedding.

The pole to the best fit great circle girdle for poles to intrabed cleavage surfaces is nearly parallel to the fold hinge defined by the Π circle (figure 12). This correlation suggests that, unlike interbed cleavage, intrabed cleavage formed during folding specifically to accommodate fold related strain. Crosscutting relationships support this argument. Although intrabed cleavage regularly cuts interbed cleavage, intrabed cleavage cuts or offsets veins as often as it is cut by them. Clearly, fold-related strain accommodation involved intrabed cleavage both genetically and developmentally.

Whereas in some beds interbed cleavage dominates strain fabric, other beds display intrabed cleavage in varying intensities, often to the degree that intrabed cleavage obscures interbed cleavage. This cleavage selection correlates directly to lithology (Figure 13). Strain accommodation during folding either occurred along pre-existing interbed cleavage surfaces or prompted the development of new intrabed cleavage surfaces. Pressure solution seams develop at lower T and P in regions of relatively high clay content because of the physico-chemical character and high surface area of clays that allows them to adsorb water and enhance diffusion (Marshak and Engelder, 1985). A combination of organic material and clays, which constitute selvage in pressure solution seams in this fold, probably had the same effect. As selvage seams develop into a network, they aid draining of cations from the seams by fluid infiltration (Marshak and Engelder, 1985). Moreover, rocks of smaller dominant grain

Figure 13: Intrabed cleavage formed easily in muddier laminations of finer dominant grain sizes.

Figure 14: Intrabed cleavage off

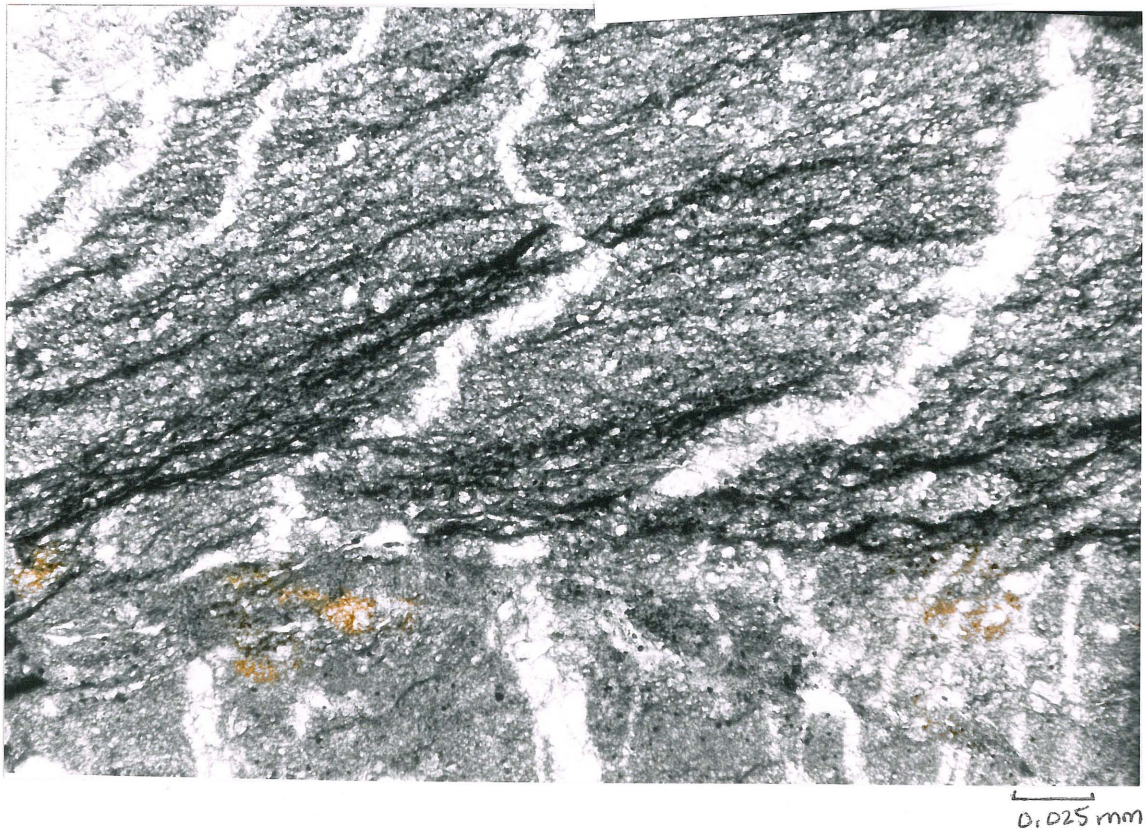

sizes experienced pressure solution at lower T and P (Elliott 1972; Rutter, 1983). Thus, at low T and P, new pressure solution surfaces did not form in the arenites, and fold-related strain pirated pre-existing interbed cleavage surfaces. In the mud-rich lutites, intrabed cleavage formed.

Intrabed cleavage accounts for extensive strains confined to individual beds. These cleavage surfaces originated as microscopically rectilinear surfaces of selvage material. Where intrabed cleavage surfaces offset vein material (Figure 14), rotating veins back to their original trends shows that intrabed cleavage originated as 1 mm to 1 cm long seams at 45° to 75° angles to bedding . The strain path that these seams accommodated depends on the lithology of the bed. As simple shear strain intensified in beds of homogeneous lithology, microscopic pressure solution seams grew and connected to create sets of parallel surfaces that traversed the entire bed. The resulting structure is a flaggy, disjunctive cleavage (Marshak and Engelder, 1985).

In beds showing significant lamination by grain size and clay content, intrabed cleavage surfaces originated in the finer-grained or clay-rich layers. As in lithologically homogeneous beds, the seams originated at oblique angles to bedding. As simple shear strain intensified in laminated beds at dips greater than 10°, the cleavage surfaces could not link together because of the intervening more competent laminae, which develop pressure solution seams only at higher stresses. Instead, interbed cleavage intensified only within less competent laminae. As folding rotated the confining limbs, interbed rotated relative to bedding by dissolution; the

surfaces rotated into orientations at smaller angles to bedding. This shearing consistently reduced bed thicknesses and rock volume.

With further strain, the sheared cleavage rotated into a thick seam that is bed-parallel and contains only selvage material (figure 15). Because this surface lacks the coherence of the parent rock, it accommodated further shear by bed-parallel slip. Slip resolved along these surfaces generated lenses of calcite-fiber slickensides (Figure 16). Thus, in finely laminated beds, pressure solution produces bed-parallel solution seams that are genetically deformational rather than diagenetic. This phenomenon illustrates the hypothesis asserted by Arthaud and Mattauer (1969) that the local direction of maximum compressive strain determines the orientations of surfaces of pressure solution, slip, and extension by reprecipitation. In this case, intrabed cleavage surfaces formed normal to compressive strain. As the limb rotated these surfaces, they accommodated shear and then slip. Further rotation allowed for extension and precipitation of calcite within the zones of slip.

Clearly, the term intrabed cleavage refers to a wide variety of pressure solution structures generated by folding strain. Intrabed cleavage produces a divergent cleavage fan around the hinge in some beds, slickensided bed-parallel selvage seams within others, and crenulations in the intensely deformed hinge region.

Fibrous veins

Extensional veins are common throughout the fold (figure 17), showing a preference for regions nearer the hinge than the outer limbs. Veins are .01 mm to 10 mm thick and 5 mm to 1 m long. They

Figure 15: Intrabed cleavage sheared into a bed-parallel position.

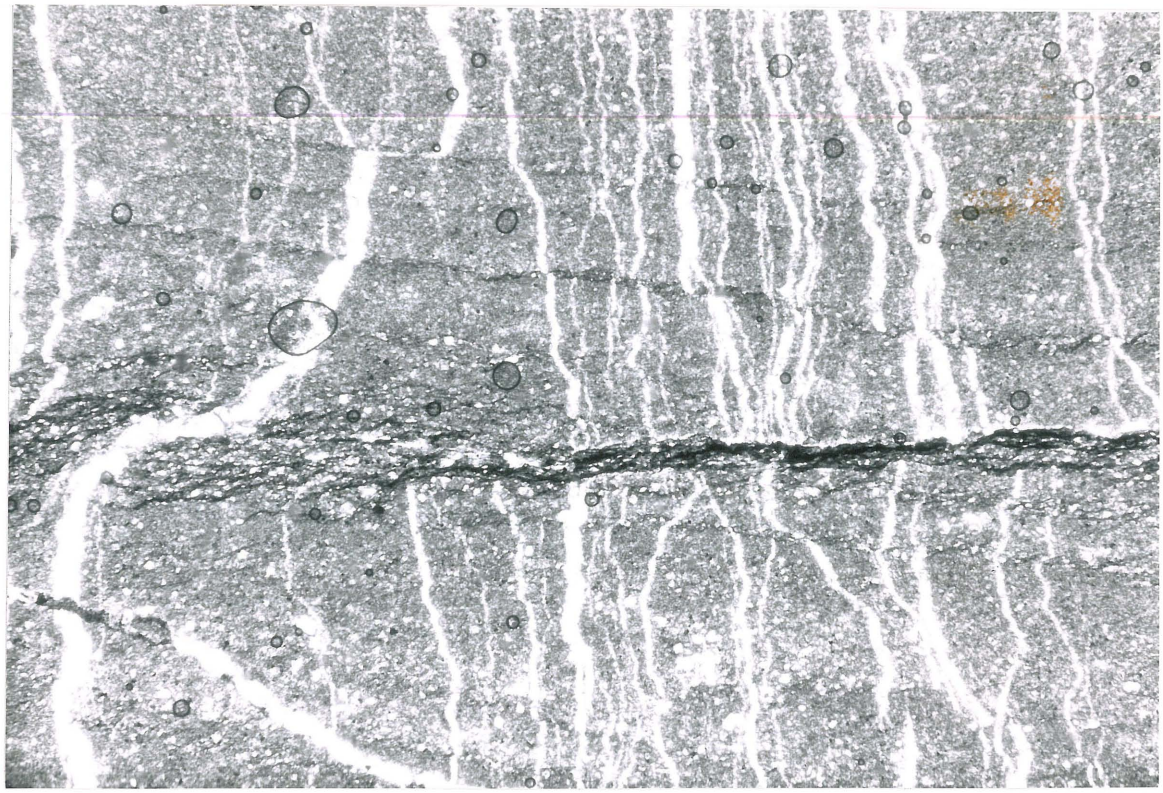

Figure 16: Calcite lenses formed by slip in bed-parallel intrabed cleavage zone.

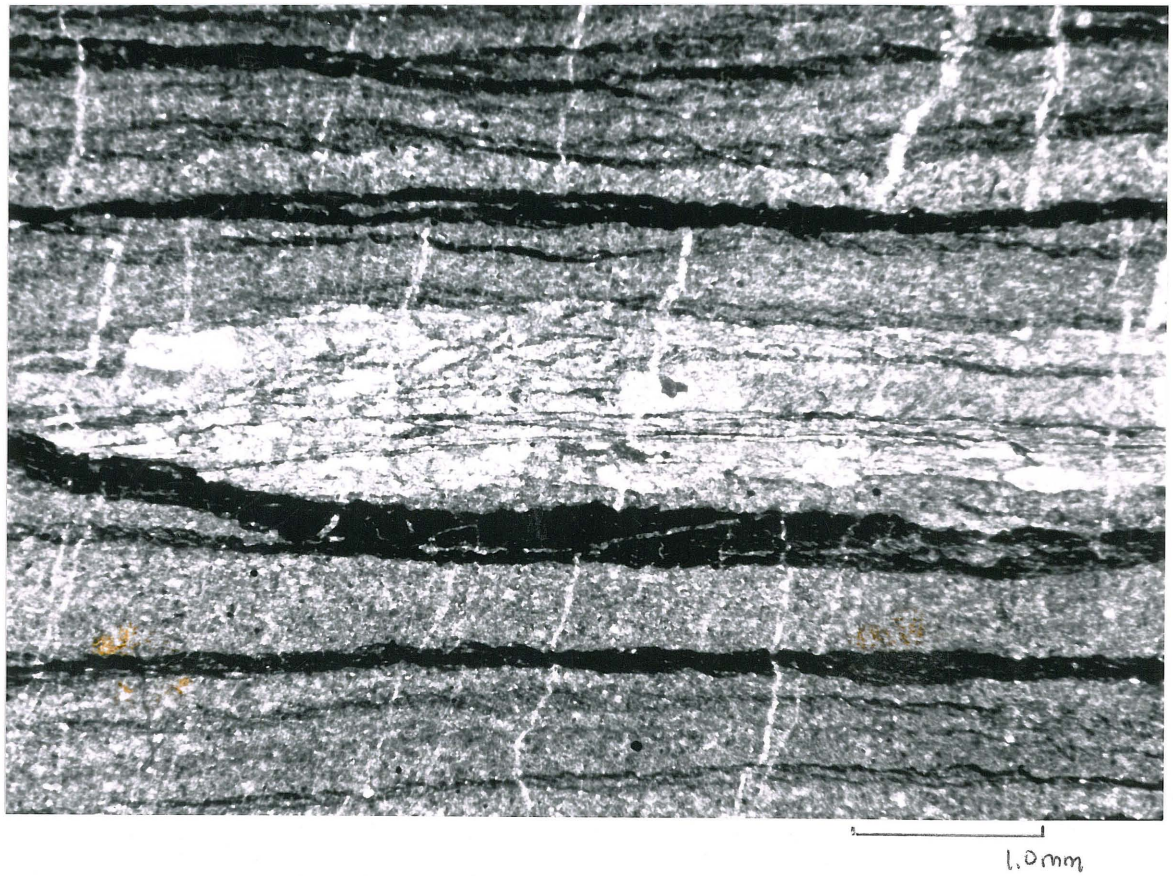

are usually normal or at large angles to bedding. Like interbed cleavage, they fan convergently about the fold. In the outer limbs of the fold, veins occasionally use interbed cleavage surfaces. Veins often thicken towards and terminate abruptly at bed slip surfaces, indicating an outer arc extension process. In general, extensional veins traverse entire competent beds, where they are spaced similarly to interbed cleavage, and only partially traverse less competent beds, where they are less intense than intrabed cleavage. Veins oriented normal to the fold axis are rare; a few exist in the hinge region and none in the limbs.

Figure 17: A weathered vein.

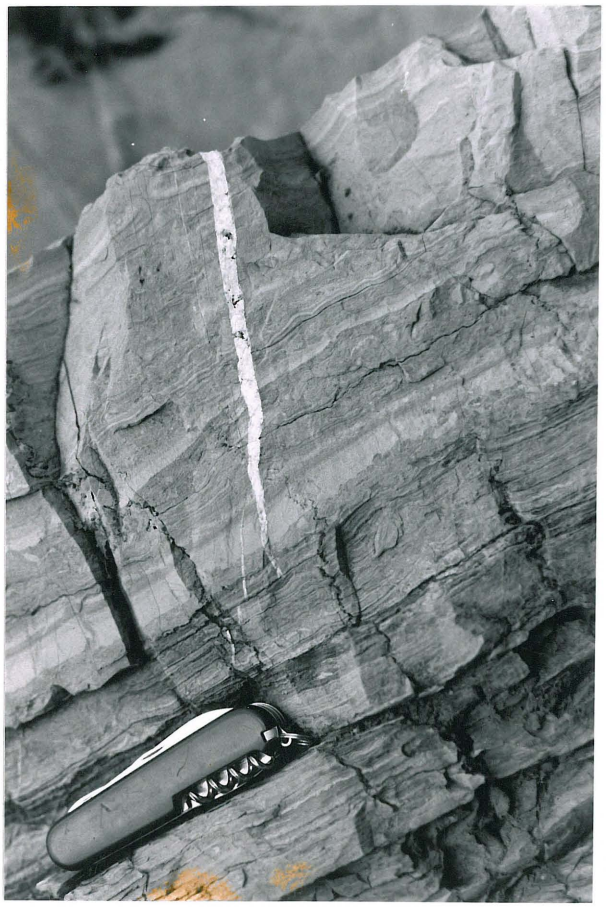

Veins have syntaxial calcite fillings, with rare crystals of fluorite. In some veins, blocky calcite crystals replace the syntaxial fibers towards the center of the vein; this either indicates recrystallization or a speeded opening of the vein. In veins offset or cut by cleavage, fibers bend or twin weakly to accommodate strain. In intensely deformed regions, large veins contain selvage seams that

connect with selvage seams in the wall rock. These veins also contain lenses of wall rock, which, during the formation of pressure-solution cleavage that cuts the vein, dissolved into intra-vein selvage seams.

A stereographic projection of poles to vein surfaces defines a great circle whose pole lies in the same plane as the hinge surface but dips to the south (figure 18). A cursory look at the scatter plot shows that these surfaces are poorly constrained when compared to other mesoscopic structures. If these veins had formed in response to outer arc extension, the great circle girdle would parallel the Π circle (Ramsay, 1967). Instead, the great circle diverges from the Π circle by 30°. Muecke and Charlesworth (1965) observe similar anomalous joint sets in intensely deformed folds in the Cardium sandstone in southwestern Canada.

Figure 18: Poles to veins.

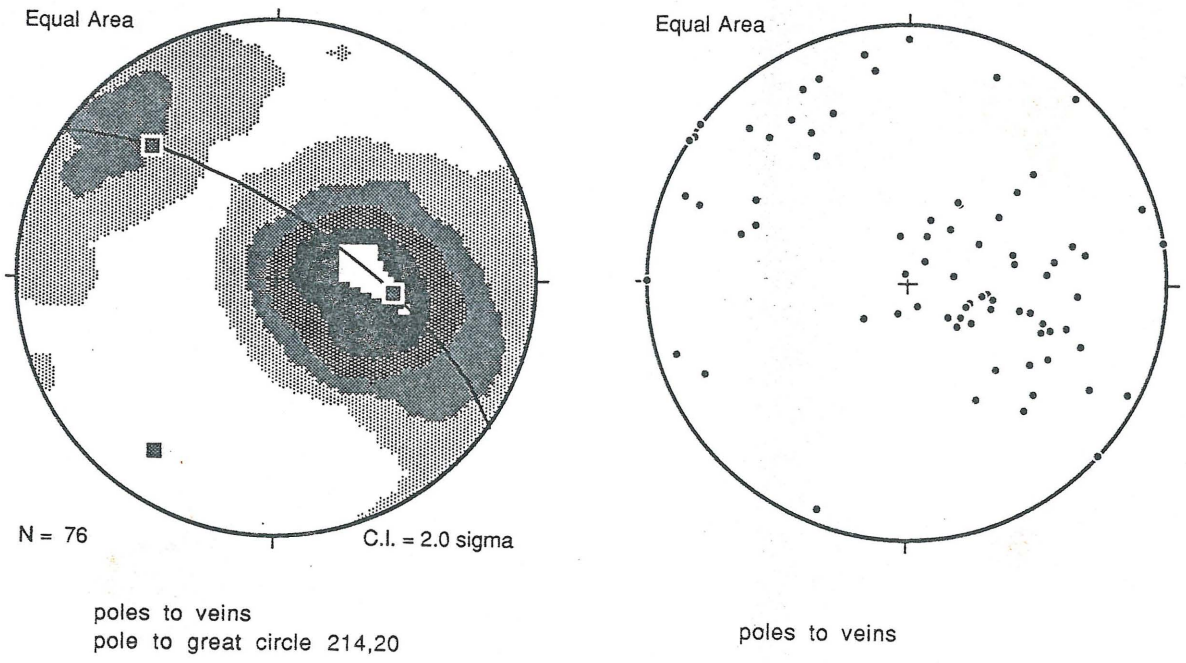

The origin of these veins is unclear. Two general possibilities are: 1) these veins, like interbed cleavage, record a deformation event other than folding; and 2) the veins accommodate a type of fold-related strain that differs from outer arc extension. As emphasized above, the absence of distinctive and generalizable cross-cutting relationships between veins and intrabed cleavage suggests that the former explanation is unsatisfactory. Cross-cutting relationships indicate that both veins and intrabed cleavage are, in general, chronologically simultaneous over a large span of time and related to the process of fold formation. Thus, a separate deformational event does not explain the vein orientations.

The latter option seems to be the only feasible explanation for this data. Hancock (1985) argues that the orientation of joint sets within folds reflects the relationship of stress to the tensile strength of the deforming rock. At low stress, veins form parallel to the hinge in typical outer arc extension structures. During higher stress, veins form to accommodate hybrid shear (figure 19). The morphology of hybrid shear joints, argues Hancock, reflects extension, but these veins form in odd orientations. Veins in the fold on Martin Mountain may reflect a hybrid shear jointing process.

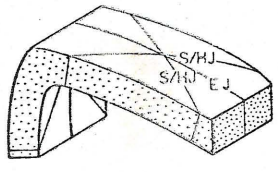

Figure 19: Orientations of hybrid shear joints (S/HJ) on a fold limb. Hinge-normal joints (EJ) are rare in this fold. (from Hancock, 1985).

En Echelon Vein Arrays

En echelon vein arrays exist only in the hinge region, at bed-dips of 0° to 30° . The vein arrays are 10 cm to 1 m long, and individual veins are 3 cm to 30 cm long. Individual veins have syntaxial fibrous calcite fillings, usually with curved fibers that indicate shearing within the vein during opening. In some cases, small vein arrays occur in tandem with intrabed cleavage; veins normal to intrabed cleavage accommodate extension normal to compression during cleavage formation.

The larger and longer vein arrays originate near broken hinges (see Figure 26d; Ramsay, 1987). Fault surfaces within these beds display slickensides and fault brecciation; they occur at large angles to the hinge surface. Thick, shaly beds surround the two competent beds which fault in the hinge. Shear zones in the surrounding, less competent beds accommodate offset produced by these faults and are characterized by long en echelon vein arrays. These vein arrays often branch, but a stereographic projection of poles to the vein arrays shows that they, like their parent faults in the hinge, lie at large angles to the near-vertical hinge surface.

Strain Distribution and Layer Rheology

Wojtal (1989) argues that discontinuous structures reflect homogeneous deformation when they are evenly spaced and show regular offsets. This fold formed both by flexural slip and by flexural flow. Slip surfaces, cleavage, and veins, however, are all evenly-spaced and locally show consistent offsets; local strain is homogeneous. The spacing of cleavage seams and the volume of rock

removed along each seam determine the net shortening due to cleavage formation; the width of veins determines the local elongation during deformation. I used the method outlined in Wojtal (1989) on seven sections cut parallel to the fold profile plane. Plots of displacement versus position within the sections indicate that displacement gradients are approximately constant and that strains are approximately homogeneous. Figure 20 gives the measured strain values (for discussion of calculating offsets, see "Methods").

Within individual beds, intrabed cleavage accommodated shear strains in areas of limb-dips from 0° to 40°, with the more intense shear strains in less competent beds with limb-dips between 10° and 30°. Shear strains in limbs outside of the angular hinge region indicate that the angular shape developed during later stages of folding, perhaps during late flattening (Ramsay, 1967). Thus, shear strains in the limbs developed in a rounded fold that later matured into an angular fold with long, straight limbs. Early interbed cleavage provides a 10% shortening strain throughout the fold, irrespective of location within the hinge or limbs. Mineral-filled veins, although common throughout the fold, occur most commonly in the hinge region, where vein growth counteracts somewhat shortening and shearing strains.

Calcite deforms easily by both pressure solution and twinning (Rutter, 1976), and, if temperatures are sufficiently high, dislocation creep may contribute to the deformation. The co-existence of twins and undulose extinction in the larger calcite grains in the limbs of the fold suggests that all three deformation mechanisms contributed to the deformation in these rocks. Because

Figure 20: Strain within beds: hand sample strains overlaid on a fold profile and corresponding Mohr diagrams.

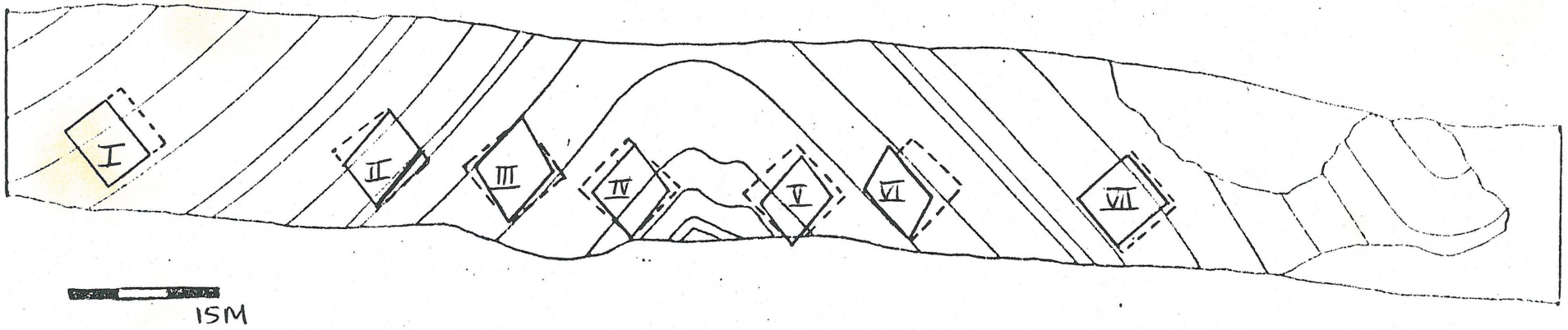

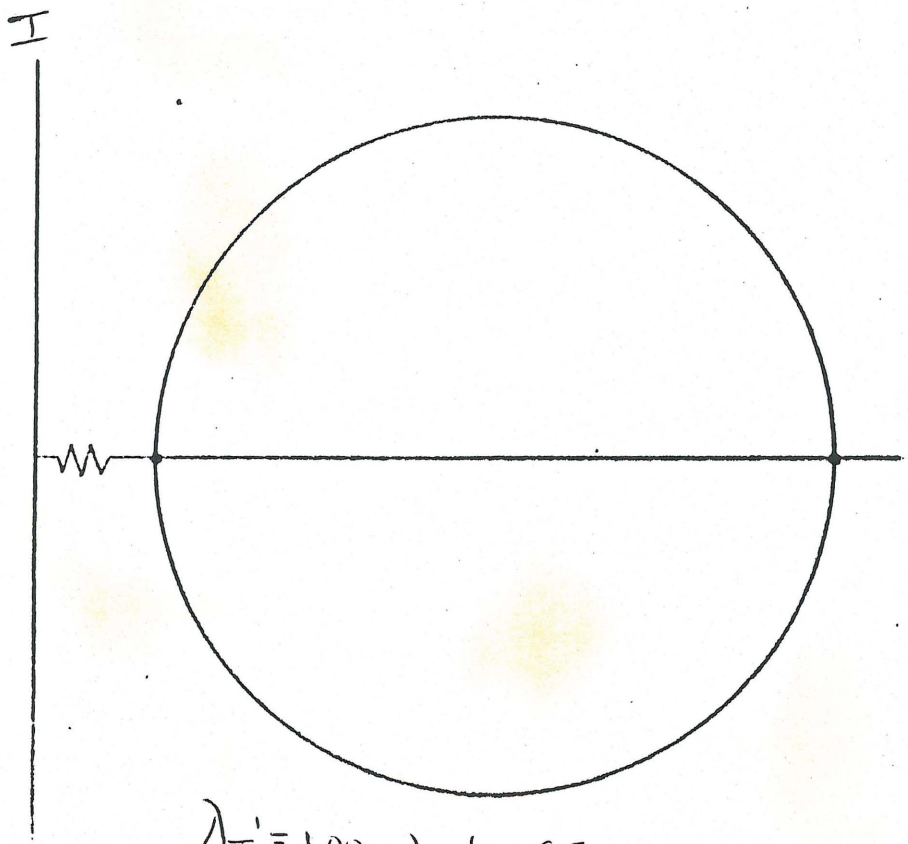

$\lambda_I' = 1.00$ $\lambda_{II}' = 1.85$
axial ratio: 0.74
area ratio: 74%

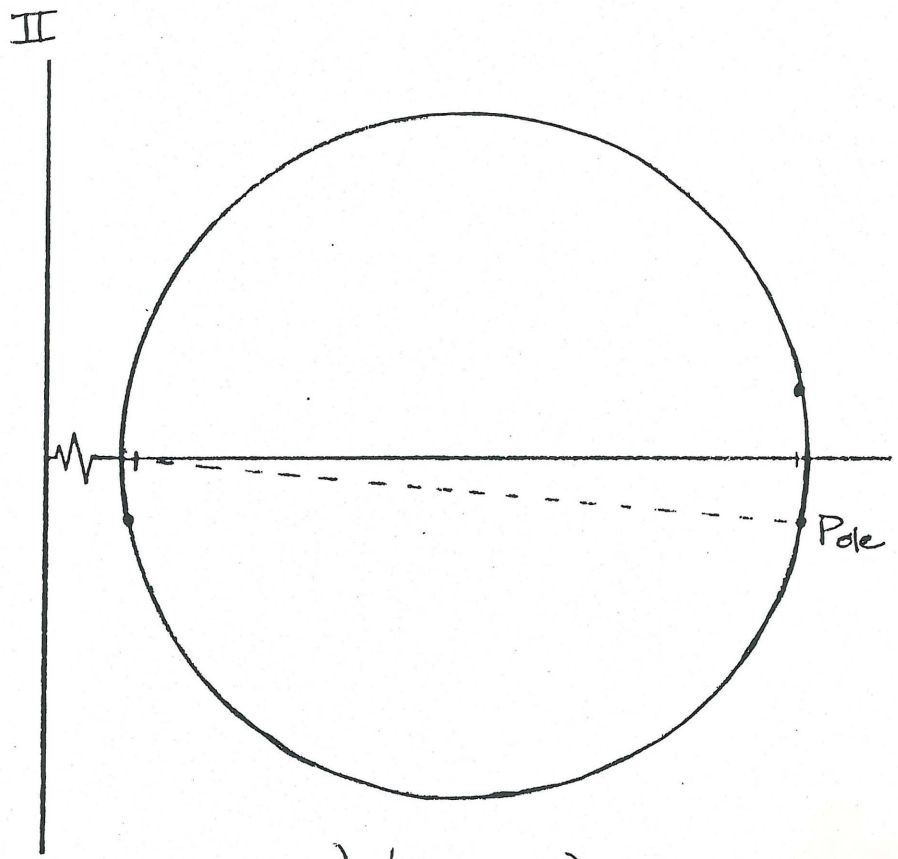

$\lambda_I' = 0.79$ $\lambda_{II}' = 1.71$
axial ratio: 0.68
area ratio: 86%

III

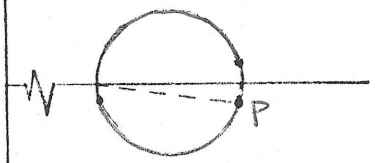

$\lambda_I' = 1.17$ $\lambda_{II}' = 1.36$
axial ratio = 0.93
area ratio = 79%

IV

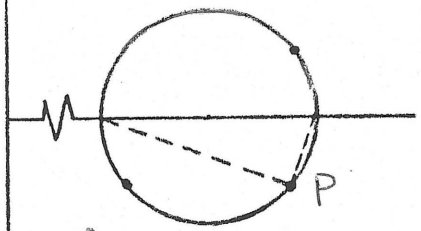

$\lambda_I' 1.17$ $\lambda_{II}' = 1.44$
axial ratio = 0.90
area ratio = 77%

V

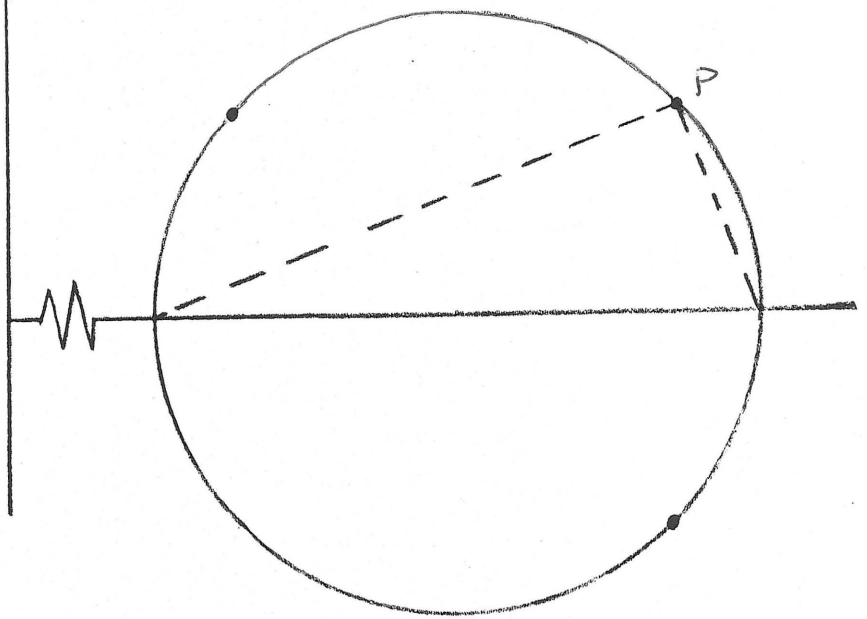

$\lambda_I' = 1.24$ $\lambda_{II}' = 2.00$
axial ratio = 1.27
area ratio = 64%

VI

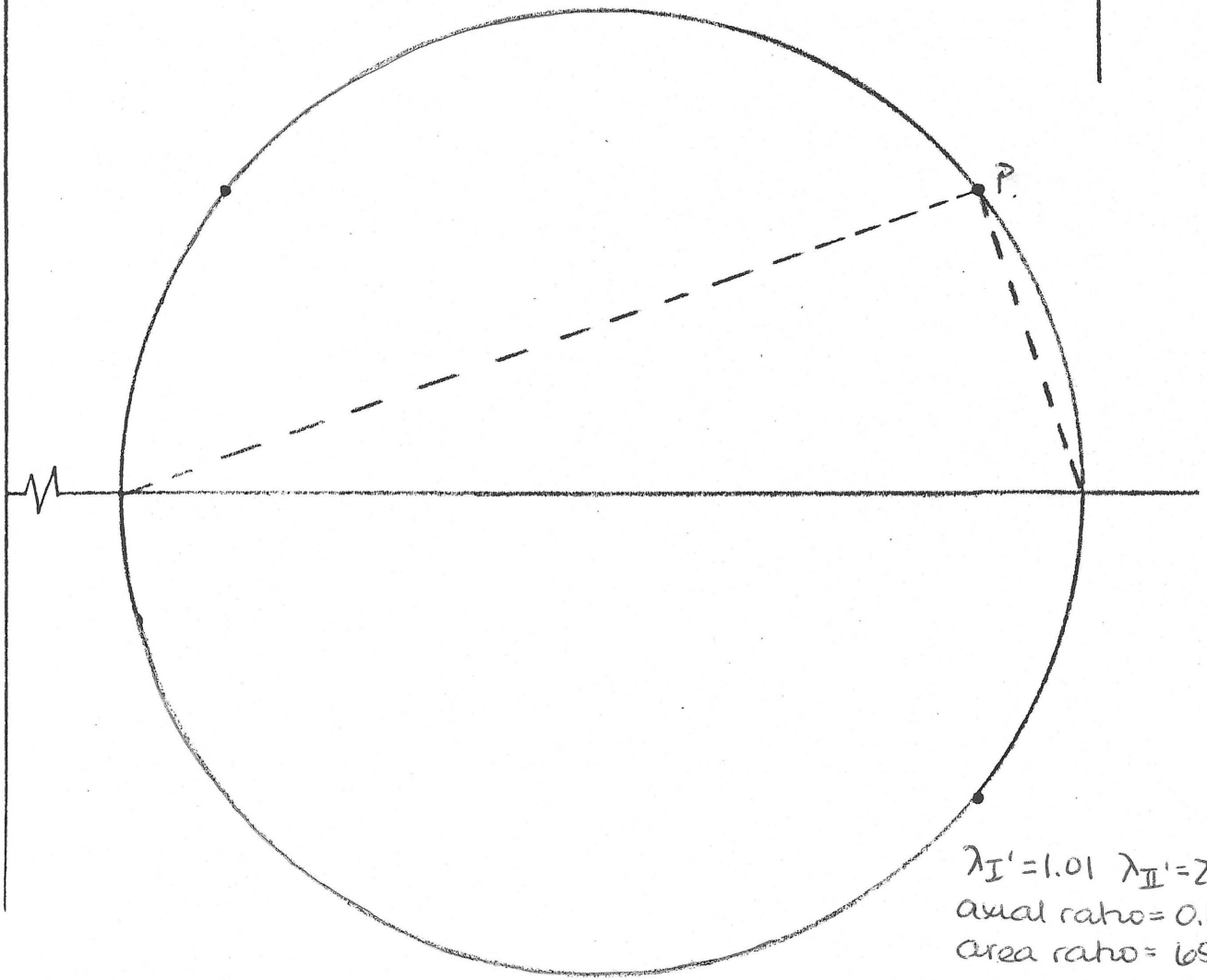

$\lambda_I' = 1.01$ $\lambda_{II}' = 2.34$
axial ratio = 0.657
area ratio = 65%

VII

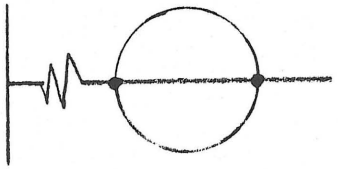

$\lambda_I' = 1.14$ $\lambda_{II}' = 1.31$
axial ratio = 0.93
area ratio = 82%

of the small grain size and muddiness of the rock, the extent of plastic behavior of the rocks remains unclear. Pressure solution and reprecipitation indicate linear or Newtonian behavior of rock during strain (Elliott, 1972). During folding, however, limbs may have exhibited both Newtonian and plastic behavior (Mitra, 1978). The structures in this fold provide a textbook example of deformational styles in the cover layer of the Central Valley and Ridge (Mitra, 1987).

Deformation History

Chronology

The genesis and evolution of cleavage within folds receives a fair amount of attention (e.g. Alvarez and Engelder, 1976; Engelder and Marshak, 1985; Helmstaedt and Greggs, 1980; Henderson et al., 1986; Marshak and Engelder, 1985; Meyer and Dunne, 1990). Most workers, including Meyer and Dunne who seem to have taken readings on Martin Mountain, argue that cleavage originates before folding as bed-normal pressure solution surfaces. As folds develop and amplify, cleavage shears in less competent beds, producing a divergent fan around the fold. In more competent beds, cleavage rotates passively with the limbs to produce a convergent fan. This model explains a common pattern of divergent and convergent cleavage fans within one fold, a pattern that the anticline here displays.

I propose above a different model for cleavage genesis in the fold on Martin Mountain. Bed-normal pressure solution cleavage formed before folding in response to a general shortening strain throughout the strata. In competent beds, folding reactivated and rotated these interbed cleavage surfaces and they remained normal to bedding. In the less competent strata, traces of interbed cleavage remain in the limbs. In general, a later set of cleavage, the intrabed cleavage, overprints the earlier cleavage. Intrabed cleavage does not necessarily reflect the shearing of the original cleavage. Two lines of evidence support the formation of intrabed cleavage during folding. Firstly, intrabed cleavage and fibrous vein sets formed

together over an extended period of time. The veins display hybrid shear orientations, an imprint of folding (Hancock, 1985). In addition, restoring veins offset by intrabed cleavage to planar orientations shows that intrabed cleavage surfaces, unlike interbed cleavage surfaces, formed at oblique angles to bedding. Thus, intrabed cleavage formed in orientations inconsistent with pre-fold shortening strain.

Secondly, stereographic projections of intrabed cleavage and interbed cleavage show that they are non-coaxial, indicating origins in different deformational episodes. Intrabed cleavage is coaxial with the fold and other fold-related structures, but interbed cleavage is not. There are two possible causes for this non-coaxiality: 1) shortening occurred on preexisting joint surfaces that formed unrelated to later shortening deformation, or 2) interbed cleavage developed in response to an early deformation event that was non-coaxial with folding. The first hypothesis is testable. If joint surfaces oblique to maximum compressive strain accommodate shortening in the form of stylolitic pressure solution, stylolitic teeth develop at oblique angles to the surface (Dean et al., 1988). The stylolitic teeth of interbed cleavage surfaces, however, developed normal to the surface. Crosscutting relationships support the second hypothesis. Interbed cleavage formed before folding produced intrabed cleavage and veins. In this fold, early cleavage in the more competent beds (interbed cleavage) rotated passively during folding. Later cleavage in the less competent beds originated during folding and, although it reflects shearing, does not reflect the shearing of originally bed normal cleavage formed before folding.

Here, I propose a history of deformation based on these mesoscopic structures :

Stage one (Figure 21a): Before tectonic deformation commenced, sediments compacted and lithified, with precipitation of calcite in pore space.

Stage two (Figure 21b): Tectonic deformation began. Sediments accommodated 1 to 10% shortening by forming evenly-spaced, bed-normal stylolites (interbed cleavage).

Stage three (Figure 21c): A second stage of deformation, non-coaxial with the first, began and folding commenced, producing a rounded, low amplitude fold. Flexural slip occurred along bedding. Competent beds accommodated shortening and shape change by dissolution along passively rotating interbed cleavage surfaces. Intrabed cleavage developed and sheared less competent beds. Fibrous veins formed.

Stage four (Figure 21d): Deformation continued and the rounded fold flattened into an angular fold. Extensional veins, bed-parallel slip surfaces, and intrabed cleavage continued to develop. Broken hinges formed, producing en echelon vein arrays.

Buckling versus Bending

Current literature on fold mechanisms generally presupposes a perspective derived from one of two predominant models; the buckling model (e.g. Currie et al, 1962; Ramsay and Huber, 1987; Hudleston, 1973) and the bending model (Suppe, 1983; Faill, 1973; Jamison, 1987). The primary distinction between the two is that buckling results from homogeneous compressive stresses normal to

Figure 21: Four stages of development in folding history.

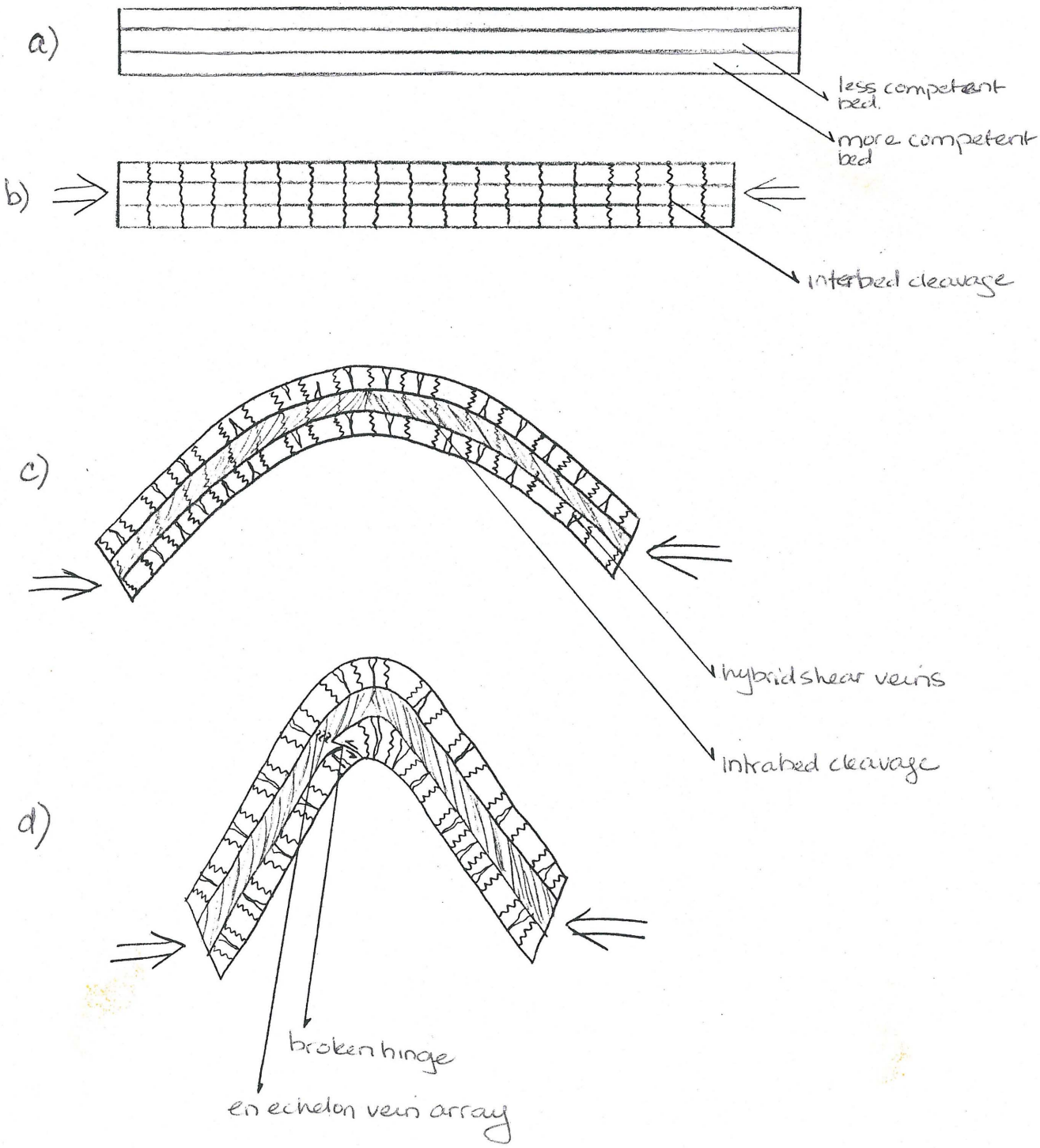

the direction of fold amplification, and bending requires a moment acting on the folded surface.

Integrating the buckle and bend fold models into an inclusive, field oriented approach to fold and thrust regions is as difficult as it is necessary. In a fold and thrust region, folding and thrusting are inherently intertwined. This does not mean that every fold must be a fault-bend fold, nor does it exclude buckle folding. Yet, it seems almost impossible to write off the effects of thrust faulting on regional map-scale folding. Tectonics in this region are indeed "thin skinned," and no map scale fold lies far enough above the thrusts and imbricates in the Cambro-Ordovician stiff layer strata that it could actually be described as deforming within a homogeneous medium. Any sizeable fold in this region will be fault related, however indirectly. Suppe (1983) writes:

> Many large-scale folds that have formed at shallow crustal level, above the brittle-plastic transition, have origins that are intimately related to slip on adjacent faults. The important classes of fault related folding include: (1) buckling caused by compression above a bedding plane decollement, (2) fault-bend folding caused by bending of a fault-block as it rides over a non-planar fault surface, and (3) fault-propagation folding, caused by compression in front of a fault tip during fault propagation.

This categorization of folds provides a good general overview of the causes of large scale folds. In addition to these types of folds, however, large scale kink folds may form during imbricate emplacement as imbricate tips displace the cover layer, producing a kink hinge (Faill, 1973).

Unfortunately, the art of distinguishing between these different types of folds in the field and without an accurate map of nearby

fault structures has not been well cultivated in the literature. A number of studies (e.g. Currie et al, 1962; Hudleston, 1973; Hudleston and Holst, 1984; Hudleston 1986; Jamison, 1987; Suppe, 1983; Suppe,1984) emphasize that shape is an important indicator of fold genesis. Perfectly rounded, sinusoidal shapes are classic illustrations in papers on buckle folds, but this is mostly due to idealized experiments and to the relatively small scale at which buckle folds have been proven to form. At the other end of the spectrum, fault propagation folds and fault-bend folds are usually drawn using kinks and chevrons instead of more curved hinge zones. This style, however, predominates because it makes the mathematics of section balancing much easier to visualize. Fold shape should not be ruled out as a possible indicator of fold genesis, but stylistic representations of folds in the literature are constructed more to reflect the theory and methods behind them than to correspond to true fold shapes in nature.

In general, the furor over buckle folds was generated in the laboratory. Documentation of natural buckle folds usually refers to hand sample size, single layer folds (Hudleston, 1986). Larger and more complex folds are inferred to be buckle folds if their geometries correspond to analogous folds created in the lab. Two admirable papers of this nature are Currie et al. (1962) and Dubey and Cobbold (1977). Currie et al. (1962) use wavelength and the thickness of a dominant member to correlate natural buckle folds to single layer buckle folds created in the laboratory. Currie et al. integrate folds of small and large scales into one model, but their

equations and predictions refer only to single layer folds that are relatively undisturbed by other structure.

Dubey and Cobbold (1977) address multi-layer buckle folds that develop by flexural slip. They combine laboratory work with field work to describe this phenomenon. Although incipient buckle folds may well be rounded, late-stage buckle folds may also be chevron shaped or box shaped. This argues in favor of Ramsay's (1967) hypothesis that chevron shaped folds generally originate as rounded folds and mature into chevrons in the late stages of folding. It also shows that pure buckling can produce a surprisingly wide range of fold shapes that depend more on specific geometric relationships with neighboring folds than on the mechanism of buckling itself. Strain in buckle folds occurs around a pinned hinge region, which does not migrate during folding (figure 22a; Ramsay, 1987). Shearing occurs in the limbs during fold amplification (Currie et al., 1962).

Folds produced by bending include kink folds and fault-bend folds. Suppe (1984) argues that fault propagation folds form by bending. Tip-line folds may initiate as buckles above a detachment, in which case strains in the fold should correspond to those in buckled layers. Models for fault propagation folding, however, hinge on models for thrust fault systems (Elliott, 1976; Suppe, 1983, Jamison, 1987; Fischer and Woodward, in press). Thrust growth may occur in three stages: a buckle above a detachment surface, the overturning of the fold and the migration of the fault through the overturned limb, and thrust movement. During the overturning of the fold, strain concentrates in one hinge (Jamison, 1987). The kinetic model that

links thrusts to fault propagation folds is elegant in its simplicity but questionable in its widespread applicability (Fischer and Woodward, in press). The term fault propagation fold, however, implies a genetic inference of an extended faulting process. Dunne et al. (unpublished) document fault propagation folds on the outcrop scale, but no documentation of map-scale fault-propagation folding exists. In any case, fault propagation folds require a proximal fault surface (figure 22b).

Kink folds result from differential stress along a surface (Faill, 1973). Extremely angular hinges and straight limbs characterize kink geometry (figure 22c; Suppe, 1984). Strain in kink folds consists of a deformed narrow hinge, slip along bed-parallel surfaces, and asymmetric patterns of slip and strain across the kink axis (Faill, 1973).

Fault-bend fold theory grows out of the observation of large scale folds in nature (e.g. Suppe, 1983). Field data that illustrate fault bend folds consist wholly of seismic sections and the observations of map scale structures in unusually good exposures. During thrusting, sedimentary strata move over thrust ramps, producing a migrating fold axis in the thrust sheet (Suppe, 1983). Clearly, fault bend folding requires an asymmetric ramp surface. Strata that have migrated over the ramp and strata that remain on the ramp show different types of strain, providing for an asymmetric fold (figure 22d; Suppe, 1983). Moreover, fault bend folds in a thrust sheet must lie directly above a fault surface and ramp.

Figure 22: Fault geometries typical of a) buckle folds, b) fault propagation folds, c) kink folds, and d) fault-bend folds. The dashed line is the fold axis.

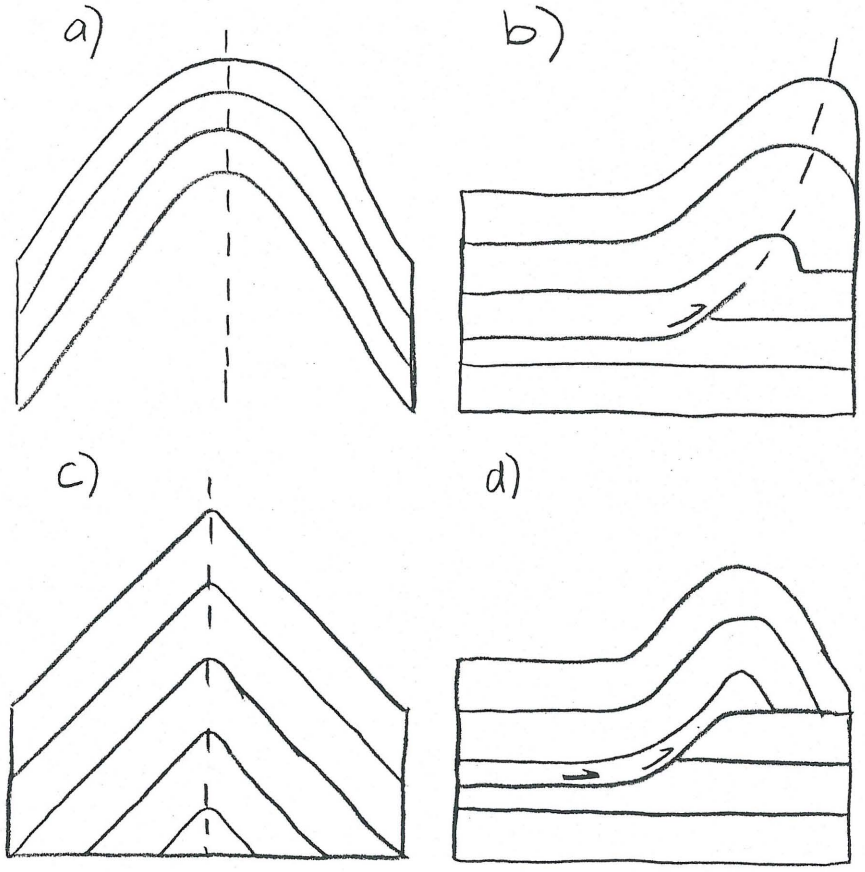

From this discussion, a set of criteria for distinguishing between buckle and bend folds emerges. Firstly, the geometric setting of the fold in relation to other structures is of primary importance. For example, a fault-bend fold must lie above a fault ramp and a buckle fold must exist in a relatively homogeneous medium. Secondly, buckle folds create symmetric strain around the pinned hinge region. Bending folds produce asymmetric strain around the hinge. Fault bend folds produce this asymmetry by differential migration over a ramp surface. Kink folds produce this asymmetry because each limb bends without respect for the other.

Geologic Setting for Deformation

The primary task of constructing a geologic setting for the anticline on Martin Mountain lies in determining what type of fold it is, correlating its formation to regional geologic structure, and examining some of the regional implications of the structures studied in the fold itself. In the Central Valley and Ridge, map-scale fault bend folds, kink folds, and fault propagation folds are well documented (Woodward, 1989). In the Cambro-Ordovician stiff layer, imbrication on thrust ramps produces fault bend folds (Geiser, 1988). Imbricate tips disturb the cover layer, creating large anticlinoria and synclinoria by a kinking mechanism (Faill, 1973). Fault propagation folds exist above regional splays from the detachment surfaces (Mitra, 1987).

The two criteria set forth for discussing fold mechanism are geologic setting and strain symmetry around the hinge. The local structural setting of this fold is visible at the outcrop. On Martin

Mountain, no large scale faults are visible, although small faults developed in the limbs of the fold as broken hinges. The outcrop studied, however, reveals only 30 m of vertical exposure. A quarry excavated recently in Martin Mountain reveals over 100 m of the fold in the Tonoloway (figure 23). If the anticline were a fault bend fold, it would lie directly above a thrust surface; if it were a fault propagation fold, a ductile extension of strain accommodated along a fault offset, a significant fault would lie below. No such fault exists either at the outcrop or at the quarry. Moreover, no such fault exists on the regional map (DeWitt and Colton, 1964).

Figure 23: Quarry view of fold.

My analysis of microstructure and mesostructure provides a firm basis for evaluating the second criterion for determining the fold mechanism, strain symmetry around the hinge. Cross cutting

relationships and data from stereographic projections show that intrabed cleavage, veins, and bed-parallel slip surfaces formed during folding. Intrabed cleavage consistently indicates that, on both limbs of the fold, beds sheared towards the hinge. These cleavage surfaces create a divergent fan around the fold surface, intensifying towards the fold hinge. Intrabed cleavage is slightly more intense in the western limb of the fold, but it is penetrative on both the hand sample and microscopic scales in the shaly strata of both limbs. Bed-slip surfaces are spaced similarly on either limb of the hinge, and offsets of top towards the hinge occur on these surfaces in both limbs. Fibrous veins, also, are symmetric about the hinge. Thus, fold-generated deformation is symmetric about the hinge axis.

The lack of a proximal fault and the symmetrical nature of strain around the hinge suggest that buckling produced this fold. The existence of a train of folds of similar wavelength in the cover strata to the east (DeWitt and Colton, 1964) supports this argument. Buckling often produces groups of buckle folds of a characteristic wavelength (Currie et al., 1962). A cross section of the area (figure

Figure 24: Highly schematic local cross section. The fold on Martin Mountain (follow dark arrow) is east of the Wills Mountain anticline and the Tussey anticline and above a duplex in the stiff strata which forms the Broadtop Block and the Wills Mountain block.

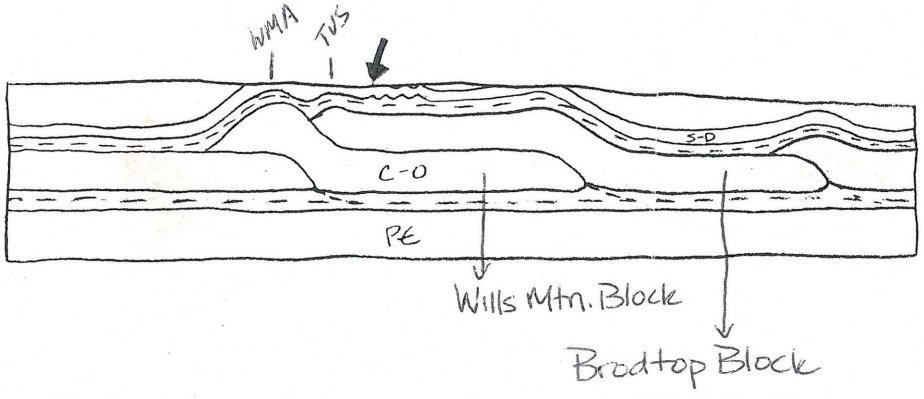

24; DeWitt and Colton, 1964; Woodward, 1985) reveals that the folds lie directly east of the Tussey anticlinorium and above a flat in the stiff layer. Here, the duplex of the Wills Mountain block and the Broadtop block flattens. The Martinsburg shale provides the detachment surface above which buckling occurred. During thrusting in the stiff layer, cover layer buckling occurred in horizontal strata that were de-coupled from the stiff layer.

Structure in this fold developed in two non-coaxial deformational episodes. The first produced interbed cleavage. The second event produced an anticlinal fold. At least two scenarios explain this non-coaxiality of structure: 1) Interference unrelated to the regional stress field by neighboring buckle folds, and 2) non-coaxial stresses caused by sequential imbricate emplacement.

The work of Dubey and Cobbold (1976) supports the first possibility. In experiment, trains of buckle folds often produce anomalously oriented folds when buckles develop out of phase with each other. In this scenario (figure 25), strata accommodate a shortening of up to 10% in the plane experiencing maximum compressive strain before buckling commenced (Figure 25a). This shortening produced interbed cleavage. Buckle folds nucleated throughout the strata; hinge regions extended and the buckles amplified (Figure 25b). Two proximal folds were out of phase with each other, and an intermediate fold, whose axis ran oblique to the plane experiencing regional maximum compressive stress, joined the two out of phase folds (Figure 25c). Here, structures formed during folding were non-coaxial with the regional stress field because they developed around a hybrid fold axis.

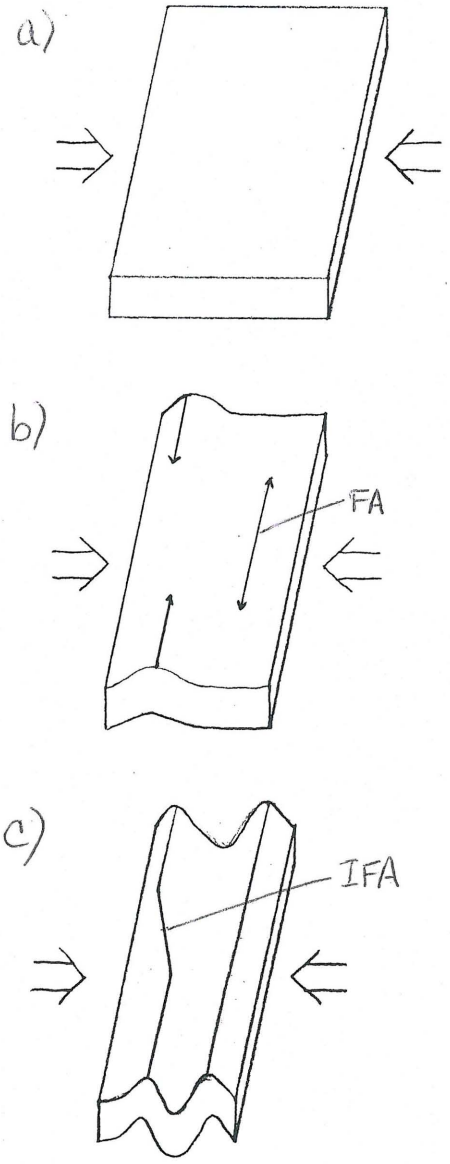

Figure 25: One model for the formation of a fold non-coaxial with early cleavage. FA = buckle fold axis. IFA = intermediate buckle fold axis.

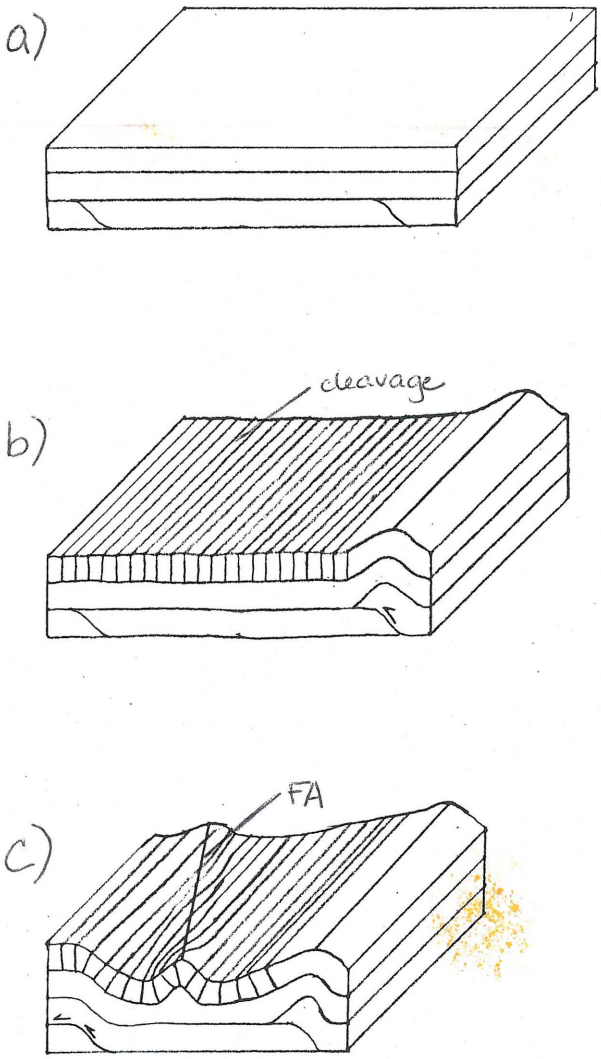

Figure 26: Another model for the formation of a fold non-coaxial with early cleavage. Cleavage is early cleavage. FA = buckle fold axis.

Perry's (1978) assertion that imbrication in the Central Valley and Ridge enjoyed an east to west structural development supports the second possibility. These buckles lie on a flat in between two anticlinoria which kinked during the emplacement of two imbricate tips (Faill, 1973). In this scenario (Figure 26), imbricate emplacement directly to the east of the region created a stress field related to imbricate and thrust ramp orientation and caused a shortening throughout the cover strata in the form of interbed cleavage (Figure 26b). Next, imbricate emplacement directly to the west of the region created a different stress field that caused buckling in the flat cover strata (Figure 26c).

Volume Loss

Introduction

In the past two decades, the topic of volume loss during low grade metamorphism has arisen in structural geology. Workers treat this topic from a variety of perspectives (e.g. Bell and Cuff, 1989; Engelder, 1984; Geiser, 1981; Etheridge, 1984; Etheridge et al., 1983; Fyfe et al., 1976; Mimram, 1977; Wright and Platt, 1982). Previously, in analyzing rocks deformed by discrete zones of dissolution and reprecipitation, structural geologists assumed an essentially closed system during deformation. Deformation involved a volume-constant process of shifting material from surfaces oriented normal to maximum compressive stress to surfaces of minimum compressive stress; the amount of material lost along surfaces of pressure solution reprecipitated locally in zones of extension (e.g. Weyl, 1959). This process involves a given amount of standing fluid through which the material diffused, driven by stress induced chemical potential gradients (Rutter, 1983). Elliott (1973) shows that this process involves a linear flow law.

Recent studies demonstrate significant volume loss strain during deformation (e.g. Engelder, 1984; Wright and Platt, 1982), challenging the assumption of essentially closed systems. Removal of rock during deformation requires an open system to accommodate mass transport by the large scale infiltration of fluids (Etheridge et al., 1984). This alternate scenario presents a number of problems for traditional theories about the mechanisms and implications of low grade metamorphism.

Etheridge et al. (1983) and Engelder (1984) attempt to calculate the fluid volumes needed to transport the significant volumes of material reported lost from many areas of deformation. The possible sources for these fluids are regional dewatering and meteoric ground water circulation. Engelder (1984) shows that in regions experiencing minor volume loss strain, the regional dewatering of lower strata accounts for fluid infiltration. In regions experiencing significant volume loss strain, he invokes the large scale circulation of meteoric water. Petroleum geologists have long been aware that meteoric water circulates as deep as 4 to 5 km within the earth's crust, the region in which low grade metamorphism commonly occurs by pressure solution phenomena. Etheridge et al. (1983) propose models of crustal water circulation. Regional lithology and regional structure, however, determine regional fluid circulation patterns. Moreover, volume loss occurs most intensely and readily in carbonates and formations of similar mineralogical composition; mineralogical variations in regional stratigraphy also influence the magnitude of volume loss strain (Engelder, 1984).

Flow laws that describe strain rates in areas experiencing pressure solution along discrete surfaces have relied on Fickian diffusion as the rate controlling factor in deformation (Weyl, 1959; Elliott 1973). But as Etheridge et al. (1984) point out, an open system during deformation mandates a reconstruction of these flow laws: "solute transport in a migrating fluid (infiltration) could give rise to significant strain rates and . . . a deformation rate equation of unfamiliar form can result which may have important

implications for crustal rheology, especially during regional metamorphism." As a result, Darcyan flow may be a more appropriate model than Fickian diffusion for these flow laws (Geiser, 1981). Engelder et al. (1983, 1984) discuss the potential roles of dissolution, pore fluid pressure, and permeability in reconstructing rate equations for regions experiencing volume loss strain.

Methods

Accurate and meaningful methods must be constructed to measure volume loss strain. Several ingenious methods use unusual gauges of strain whose original size is either known or constant. For example, Wright and Platt (1982) use strained graptolites and Engelder (1984) uses fossils such as ammonites and crinoids. Beutner (1985, 1988) uses strain around undeformable grains of metal oxides. One drawback of these methods is that they cannot distinguish between volume loss caused by compaction/lithification and volume loss caused by tectonic deformation. Another drawback is limited applicability; many deformed regions do not consistently contain markers whose original size can be known a priori or whose size can be shown to be unchanged during burial, lithification, and deformation.

Rocks without these independently known markers offer only one known state for analysis: the strained state. Estimating a change in volume between the undeformed and deformed strata requires extrapolation of the undeformed state using evidence from the deformed state. In the case of shallowly deformed sedimentary

strata such as this fold, twinning, dislocation glide, pressure solution, slip, and fibrous veins record strain. Twinning and dislocation glide, however, do not produce volume loss strain. Volume loss strain occurs along distinct surfaces of dissolution and reprecipitation such as veins and stylolites. Using these structures to infer volume loss excludes information about changes in volume during lithification and pore cementation. In addition to this, certain lithological prerequisites ensure an accurate analysis of volume loss strain using only discrete zones of dissolution and reprecipitation. Firstly, low porosity before deformation excludes reprecipitation in pore cavities during deformation. Measuring the volume of pore cement material is difficult, and distinguishing between diagenetic and deformational pore cements is near impossible. In this section of the Tonoloway, small dominant grain sizes ensure that porosity was originally low and diminished further during lithification and compaction.

Secondly, a firm understanding of the origins and development of the structures is necessary. Otherwise, surveys of volume loss strain might include pre-deformation fabrics, such as bed-parallel diagenetic stylolites. All of the structures in this fold in the Tonoloway relate to two deformational events, pre-fold shortening and folding. Thus, volume loss estimates based on these structures reflect only volume loss resulting from tectonic strain.

In the fold on Martin Mountain, volume loss strains occurred on interbed cleavage, intrabed cleavage, extensional vein, en echelon vein array, and slickensided bed-parallel slip surfaces. These structures fall into two categories: areas where calcite precipitated

in veins or slickensides and areas where calcite dissolved along pressure solution seams. Volume loss strain did not occur in areas that do not contain these structures. Volume loss can either be measured directly as the difference between volume gained in areas of precipitation and volume lost in areas of pressure solution, or it can be measured indirectly from strain.

Veins convey information about offset and change in volume through their size and fibers. Geometric relationships between microlithons and selvage seams also convey volume loss information. In toothed pressure solution surfaces, minimum offset equals the length of the longest stylolitic tooth (Ramsay and Huber, 1983). With seams oblique to bedding, offset normal to seams equals the estimated separation of the microlithons necessary to reestablish bedding continuity. If well-preserved fossils of a characteristic size or shape show partial dissolution along a seam, offset is at least as great as the missing part of the fossil. These measurement techniques assume no slip along selvage surfaces unless slickensides indicate movement.

Offsets measured in two dimensional space (such as thin sections and cut hand samples) approximate three dimensional conditions if the structures under consideration all run roughly normal to the surface measured. If, for example, cleavage trends parallel to the fold axis, veins trend normal to the fold axis, and slickensides parallel bedding, no section can fairly represent total volume loss strain. In the fold on Martin Mountain, however, sections cut parallel to the profile plane include all structures.

Field work and rudimentary lab work provide three scales for analysis: thin section, hand sample, and outcrop. An accurate estimate of total volume loss strain within any region requires analysis on a scale at which all of the structures are penetrative. Unfortunately, scale presents an insurmountable obstacle to accurately measuring volume loss strain in this fold because of the consistent disparity between scales at which interbed cleavage and intrabed cleavage are penetrative. Interbed cleavage is evenly spaced and mesoscopically penetrative. Intrabed cleavage manifests itself on both the mesoscopic scale, as a divergent cleavage fan in less resistant beds, and the microscopic scale, as asymmetric crenulations. A survey of volume loss strain on the hand sample scale neglects microscopic intrabed cleavage, and a survey of volume loss strain on the thin section scale neglects interbed cleavage. The accurate assessment of volume loss strain requires an overwhelming effort to integrate information from thin sections with information from hand samples using a wide range of both types of samples. Here, a survey of a limited number of thin sections and hand samples provides an introductory investigation into volume loss strain.

Change in Area in Thin Section

Thin sections from six samples in a variety of locations within the fold (two from the far western limb, two from the mid limb, and two from the hinge) cut normal to both bedding and structures indicate volume loss (Figure 27).

Ao = the unstrained area represented by each thin section
Ad = the area of the deformed thin section
Av = the total area of vein material in the thin section
Ap = total area presumed lost along pressure solution seams
ΔA = percent area loss represented by each thin section

The original undeformed area represented by each thin section is:

$$Ao = Ad - Av + Ap$$

The difference between area of undeformed section and deformed section is:

$$\Delta A = 100\% - Ad/Ao$$

The margin of error in these estimates is high because many samples show thin zones of asymmetric crenulation cleavage. Measuring the offset along each surface is impossible, but the spacing of some of the thicker seams provides for an approximation of loss. Thus, these figures involve a 10% margin of error. Thin sections show up to a 10% loss in western limbs dipping between 40° and 50°, a 10% to 30% loss in western limbs dipping 30° to 40°, and a (-5)% to 15% loss in the hinge region (Figure 27). Because strain is symmetrical across the hinge, these figures also reflect volume loss in the eastern limb.

Strain in Hand Sample

In seven hand samples cut along faces normal to the fold axis and etched for clarity of pressure solution seams, measured displacement gradients are approximately constant and strains are approximately homogeneous. Measured strains give a ratio of the area in the plane of section after deformation to the area in the plane of section prior to deformation. In these samples, where

displacements are restricted to the profile plane, the measured area ratios are equal to the ratio of volume in the deformed state to volume in the undeformed state (Figure 20). Volume ratios measured in this manner give a much broader range than the measured changes in area in thin section. Hand samples from beds dipping between 40° and 50° experienced a 15% to 35% reduction in area, beds dipping between 30° and 50° a 15% to 35% reduction, and the hinge region a 15% to 25% reduction (Figure 27).

Figure 27: Estimates of Volume Loss Strain.

	location in fold		
volume loss	far limb	limb	hinge
thin section	0 - 10%	10 - 30%	(-5) - 15%
hand sample	15 - 35%	15 - 35%	15 - 25%
volume loss strain estimate	20%	25%	15%

General Estimate of Volume Loss

Clearly, the data from thin sections and hand samples give conflicting estimates of volume loss. Although estimates from thin sections use change in area and estimates from hand samples use strain, these figures both use offset measurements. Instead, these figures show wide variations for two reasons. The first, as discussed above, is the problem of scale. The strain figures show a larger range of volume loss because they reflect the hand sample scale; at this scale, interbed cleavage, which accounts for roughly a 10% shortening (volume loss strain) is penetrative. The second problem is simply that, in this fold, volume loss strain as manifested in a variety of lithologies and fabrics cannot be accurately assessed using the small number of samples surveyed; variation within such a small number of samples is natural.

Both sets of volume loss estimates above neglect the contribution to volume change of bed-parallel slip surfaces. These surfaces average a thickness of 5 mm and occur approximately every 0.5 m; they account for 1% of the total volume of the folded rock and this 1% constitutes volume gain. Compared to the volume loss estimates within beds, this figure is negligible.

Before folding began, interbed cleavage produced volume loss strain. Although slickensides obscure the history of bed slip surfaces before folding, discontinuous bedding surfaces may have acted as sites of calcite reprecipitation during pre-fold shortening. Interbed cleavage accounts for approximately a 10% loss, but some of this loss occurred during folding. Bed-parallel slip surfaces reflect a 1% increase in volume. If pre-fold strain occurred as a

volume constant process, volume loss along bed-normal cleavage surfaces equalled volume gain in bed-parallel discontinuities. If so, early cleavage accommodated less than a 1% shortening strain before buckling. This is almost impossible. First, twinning could easily accommodate this shortening without the formation of any pressure solution surfaces (Ramsay and Huber, 1983). Second, experimental work (e.g. Ramsay, 1987; Dubey and Cobbold, 1977) shows that strata accommodate a shortening of around 10% before buckling occurs. Volume loss strain occurred on bed-normal pressure solution cleavage surfaces before folding began.

During folding, volume loss strain continued as intrabed cleavage developed and interbed cleavage intensified. Volume loss strain resulting from both interbed cleavage and intrabed cleavage demonstrates that volume loss strain was equally viable as a result of both pure (interbed cleavage) and simple (intrabed cleavage) shear strains. Because volume loss occurs proportional to structure intensity, volume loss strain correlates to fold morphology and geometry (Figure 28). The persistence of interbed cleavage throughout the fold created a background volume loss strain. The far limb regions experienced about a 20% volume loss strain. In the near-hinge limbs, intrabed cleavage surfaces are more common, and about a 25% volume loss strain occurred. In the hinge, however, the effects of intrabed cleavage are mediated by volume gains resulting from extensive vein growth in the form of extensional veins and en echelon shear vein arrays. A volume loss strain of about 15% occurred in the hinge region.

Figure 28: The relationship between structures and volume loss strain.

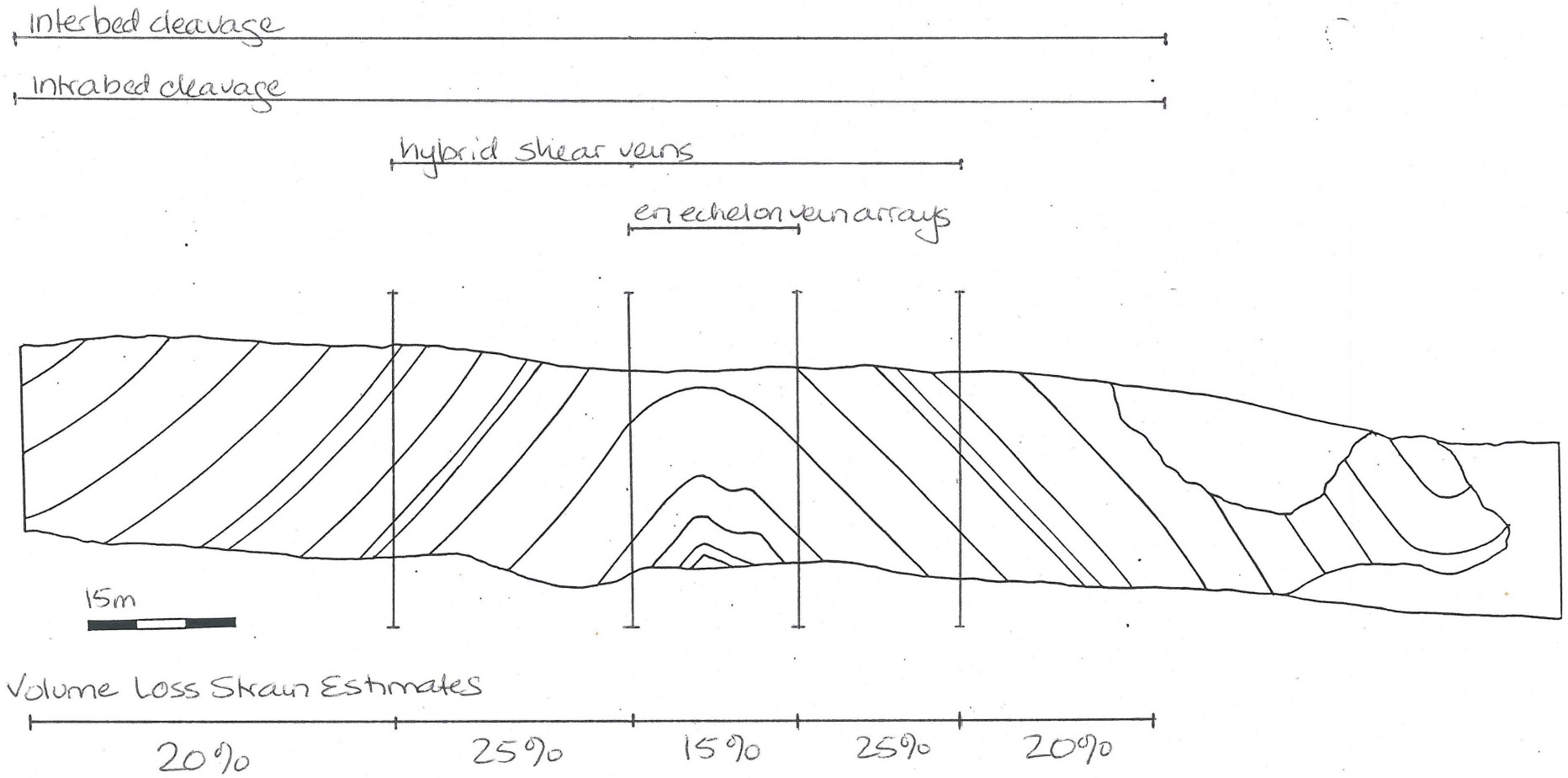

Problems of Fluid Infiltration

Significant volume loss strain in this fold raises the problem of a transporting mechanism and sink for the material. Etheridge et al. (1984) and Engelder (1984) suggest that the large scale infiltration of fluid provided either by dewatering or meteoric ground water percolation removed material from pressure solution surfaces and through fractures (preserved as veins). If this is the case, the large volume of fluid circulating through the fold passed through nearby strata and also removed some material there. This fluid gathered trace elements foreign to the Tonoloway while circulating in neighboring strata. Although the predominance of calcite within the Tonoloway excludes the nucleation of other types of minerals in veins and fluid conduits (Mitra, 1987), calcite crystals formed in this vein network should include trace elements foreign to the wall rock.

In this case, the cathodoluminescence properties of foreign vein materials should diverge significantly from the wall rock (Marshall, 1988). Carbonates usually luminesce in the range between red and orange; differences in trace ion concentrations are not spectacular (Marshall, 1988). Cathodoluminescence shows that the wall rock comprises calcite, organic material, clays, and tiny grains of quartz that luminesce light blue and constitute about 0.01% of the sediments. In all of the thin sections, the undeformed wall rock luminesces dull orange, indicating high iron content (Sippel and Glover, 1965). Selvage seams do not luminesce, and the absence of quartz grains here suggests that quartz also dissolved along pressure solution seams. Most calcite veins luminesce bright

orange because vein material is free of the organic rich clays spread uniformly throughout the wall rock. No quartz recrystallized in the veins, suggesting that fluid infiltration completely removed it from the system. Some veins, however, reveal brownish calcite crystals among the orange crystals. These darker crystals, however, are randomly oriented and spaced. They either formed by later recrystallization or reflect differences within the trace element composition of the veins. Perhaps vein fibers originally contained a record of successive calcites crystallizing, and recrystallization into blocky crystals erased this pattern in favor of a random pattern. In some samples, tiny vein networks contain only the darker glowing crystals. These veins are very thin, and perhaps reflect a mirocrack system through which fluids migrated (Geiser, 1981).

The cathodoluminescence properties of thin sections yield ambiguous results. Information in vein materials neither proves nor disproves the hypothesis that fluid infiltration occurred. The ambiguous character of vein material could indicate one of three things: 1) no infiltration occurred, 2) foreign trace elements contaminated and equilibrated with the strata before deformation and, as a result, precipitates in fractures during deformation are unremarkable, or 3) in these strata, strain during infiltration and the later recrystallization of vein materials obscured trace element evidence. The first suggestion is unlikely. If volume loss strain occurred, then the lost volume must have been transported out of the system. The accessibility of conduits in pressure solution seams and fractures supports infiltration of fluids as a more likely motor for volume loss than solid state migration of material.

The second suggestion is possible. The lack of good evidence of infiltration could reflect equilibration of foreign trace elements in the Tonoloway before deformation. Bethke (1988) shows that, in sedimentary basins, large scale fluid migration occurs during burial. Foreign trace ions from local shales and quartzites could have entered the Tonoloway in cements. These foreign trace elements could have equilibrated with the wall rock during deformation, when temperatures and pressures were relatively high. If veins crystallized during deformation trapped the same trace ions, the difference between trace ion concentrations in the wall rock and fractures is minimal. The third suggestion is also possible. Marshall (1988) and Sippel and Glover (1965) note that cathodoluminescence often gives poor results for deformed carbonates. This results from recrystallization and the general obscuration of zoning features by strain.

Probably, veins within these samples do not clearly record foreign fluid infiltration during deformation both because of the influx of similar foreign fluids during burial and because strain obscures these features. Volume loss strain occurred in the Tonoloway at the depth of about 3 km (Meyer and Dunne, 1990). This depth lies well within the 2 to 10 km range at which Etheridge at al. (1983) estimate that meteoric ground water circulates and within the 4 km range that Engelder (1984) estimates meteoric ground water circulation. Moreover, the Tonoloway lies above the sizeable Martinsburg Shale, in which Wright and Platt (1982) document a volume loss of 50%, indicating intense dewatering. The dewatering of the strata below the Tonoloway such as the Martinsburg probably

also contributed to local fluid circulation. Thus, fluids probably did circulate through the Tonoloway during deformation, providing the vehicle for the removal of carbonates from pressure solution surfaces through fractures, selvage seams, and perhaps a microcrack system.

Bibliography

Alvarez, W. et al., 1978. Classification of solution cleavage in pelagic limestones. Geology, 6: 263-266.

Alvarez, W. and Engelder, T., 1976. Formation of spaced cleavage and folds in brittle limestone by dissolution. Geology, 4: 698-701.

Arthaud, F., 1969. A graphical method for determining the shortening, elongation, and intermediate directions from a population of faults. Extrait du Bulletin de la Societe geologique de France, 7e serie, t. XI: 720-737.

Arthaud, F. and Mattauer, M., 1969. Examples of stylolites with a tectonic origin in Languedoc, their relationship with brittle tectonics. Extrait du Bulletin de la Societe geologique de France, 7e serie, t. XI: 738-744.

Bell, T.H. and Cuff, C., 1989. Dissolution, solution transfer, diffusion vs. fluid flow and volume loss during deformation/metamorphism. Journal of Metamorphic Geology, 7: 425-447.

Bethke, C., 1988. Supercomputer analysis of sedimentary basins. Science, 239: 261-265.

Beutner, E.C. and Diegel, F.A., 1985. Determination of fold kinematics from syntectonic fibers in pressure shadows, Martinsburg Slate, New Jersey. American Journal of Science, 285: 16-50.

Beutner, E.C. et al., 1988. Kinematics of deformation at a thrust fault ramp from syntectonic fibers in pressure shadows. GSA Special Paper 222.

Chapple, W.M. and Spang, J.H., 1974. Significance of layer-parallel slip during folding of layered sedimentary rocks. GSA Bulletin, 85: 1523-1534.

Cloos, E., 1971. Microtectonics along the Western Edge of the Blue Ridge, Maryland and Virginia. The Johns Hopkins Press, Baltimore, MD.

Currie, J.B. et al., 1962. Development of folds in sedimentary strata. GSA Bulletin, 73: 655-674.

DeWitt, W. Jr. and Colton, G.W., 1964. Bedrock geology of the Evitts Creek and Pattersons Creek quadrangles, Maryland, Pennsylvania, and West Virginia. US Geological Survey Bulletin, 1173.

Dahlstrom, C., 1970. Structural geology in the eastern margin of the Canadian rocky mountains. Bulletin of Canadian Petroleum Geology, 18(3): 332-406.

Dean, S.L. et al., 1988. Structural chronology of the Alleghenian orogeny in Southeast West Virginia, GSA Bulletin,100: 299-310.

Dubey, A.K. and Cobbold, P.R., 1976. Noncylindrical flexural slip folds in nature and experiment, Tectonophysics, 38: 223-239.

Durney, D.W., 1972. Solution transfer, an important geological mechanism. Nature, 235: 315-316.

Durney, D.W., 1976. Pressure Solution and Crystallization Deformation, Phil Trans R Soc Lond, A283: 229-240.

Elliott, D., 1973. Diffusion flow laws in metamorphic rocks. GSA Bulletin, 84: 2645-2664.

Elliott, D, 1976. The energy balance and deformation mechanisms of thrust sheets. Phil Trans Royal Soc Lon, A 283: 289-312.

Engelder, T., 1984. The role of pore water circulation during the deformation of foreland fold and thrust belts. Journal of Geophysical Research, 89(B6): 4319-4325.

Engelder, T. and Marshak, S., 1985. Disjunctive cleavage formed at shallow depths in sedimentary rock. Journal of Structural Geology, 7(3/4): 327-343.

Etheridge, M.A., 1984. High fluid pressures during regional metamorphism and deformation; implications for mass transport and deformation mechanisms. Journal of Geophysical Research, 89(B6): 4344-4356.

Etheridge, M.A. et al., 1983. The role of the fluid phase during regional metamorphism and deformation. Journal of Metamorphic Geology,1: 205-226.

Evans, B., 1986. Diffusion induced grain boundary migration in calcite. Geology,14(1): 60-63.

Faill, R.T., 1973. Kink-band folding, Valley and Ridge Province, Pennsylvania, GSA Bulletin, 84:1289-1314.

Ferrill, D.A. and Dunne, W.M., 1989. Cover Deformation above a blind duplex: and example from West Virginia, U.S.A. Journal of Structural Geology, 11(4): 421-431.

Fischer, M.P. and Woodward, N.B., 1990. Some thoughts on modeling the geometric evolution of thrust systems. in press.

Fyfe, W.S. et al., 1978. Fluids in the Earth's Crust. Elsevier, New York.

Geiser, P.A., 1981. Joints, microfractures, and the formation of solution cleavage in limestone. Geology, 9: 280-285.

Geiser, P.A., 1988. Mechanisms of thrust propagation: some examples and implications for the analysis of overthrudt terranes, Journal of Structural Geology, 10(8): 829-845.

Geiser, P.A., 1989.The role of kinematics in the construction and analysis of geologic cross sections in deformed terranes, GSA Special Paper 222.

Gray, D.R., 1981. Cleavage-fold relationships and their implications for transected folds: an example from Southwest Virginia, USA. Journal of Structural Geology, 3(3): 265-277.

Green, H.W., 1984. Pressure solution creep: some causes and mechanisms. Journal of Geophysical Research, 89(B6): 4313-4318.

Groshong, R.H., 1975. Strain, fractures, and pressure solution in natural single-layer folds. GSA Bulletin, 86: 1363-1376.

Hancock, P.L., 1985. Brittle micro-tectonics: principles and practice, Journal of Structural Geology, 7: 437-457.

Helmstaedt, H. and Greggs, R.G., 1980. Stylolitic cleavage and cleavage refraction in lower Paleozoic carbonate rocks of the Great Valley, MD. Tectonophysics, 66: 99-114.

Henderson, J.R. et al., 1986. A history of cleavage and folding: an example from the Goldenville Formation, Nova Scotia. GSA Bulletin, 97: 1354-1366.

Hudleston, P.J., 1973. Fold morphology and some geometrical implications of theories of fold development. Tectonophysics, 16: 1-46.

Hudleston, P.J., 1986. Extracting Information from folds in rocks. Journal of Geological Education, 34(4): 237-245.

Hudleston, P.J. and Holst, T.B., 1984. Strain analysis and fold shape in a limestone layer and implications for layer rheology. Tectonophysics,106: 321-347.

Jamison, W.R., 1987. Geometric analysis of fold development in overthrust terranes. Journal of Structural Geology, 9(2): 207-219.

Marshak, S. and Engelder, T., 1985. Development of cleavage in limestones of a fold and thrust belt in Eastern New York. Journal of Structural Geology, 7(3/4): 345-359.

Marshak, S. and Mitra, G, 1988. Basic Methods of Structural Geology. Prentice Hall, Englewood Cliffs, NJ.

Marshall, D.J., 1988. Cathodoluminescence of Geologic Materials. Unwin Hyman, Boston.

Mase, C.W., 1987. The role of pore fluids in tectonic processes. Reviews of Geophysics, 25(6): 1348-1358.

McClay, K.R., 1977. Pressure solution and coble creep in rocks: a review. Journal of the Geological Society of London,134: 57-70.

McClay, K.R., 1977. Pressure solution and coble creep in rocks. Journal of the Geological Society of London,134: 71-75.

Meyer, T.J. and Dunne, W.M., 1990. Deformation of Helderberg limestones above the blind thrust system of the central Appalachians. Journal of Geology, 98: 108-117.

Mimram, Y., 1977. Chalk deformation and large scale deformation of calcium carbonate. Sedimentology, 24: 333-360.

Mitra, S., 1978. Microscopic deformation mechanisms and flow laws in quartzites within the South Mountain Anticline, Journal of Geology, 6: 129-152.

Mitra, S., 1987. Regional variations in deformation mechanisms and structural styles in the central Appalachian orogenic belt. GSA Bulletin, 98(5): 569-590.

Muecke, G.K. and Charlesworth, H.A.K., 1966. Jointing in folded Cardium sandstones along the Bow River, Alberta. Canadian Journal of Earth Sciences, 3: 579-596.

Perry, W.J., 1978. Sequential deformation in the Central Appalachians, American Journal of Science, 278: 518-542.

Perry, W.J. Jr., and de Witt, W. Jr., 1977. A field guide to thin skinned tectonics in the central Appalachians. AAPG conference, June 12-16, 1977.

Pollard, D.D. and Aydin, A, 1988. Progress in understanding jointing over the past century. GSA Bulletin, 100: 1181-1204.

Ramsay, J.G., 1967. Folding and Fracturing of Rocks. McGraw-Hill Book Co.

Ramsay, J.G. and Huber, M.I., 1983. The Techniques of Modern Structural Geology. Volume I: Strain Analysis. Academic Press.

Ramsay, J.G. and Huber, M.I., 1987. The Techniques of Modern Structural Geology. Volume II: Folds and Fractures. Academic Press.

Rodgers, J., 1970. The Tectonics of the Appalachians. Wiley Interscience, London.

Rutter, E.H., 1976. The kinematics of rock deformation by pressure solution. Phil Trans R Soc Lond, A283: 203-220.

Rutter, E.H., 1983. Pressure solution in nature, theory, and experiment. J Geol Soc Lond, 140: 725-740.

Schwandler, H.W. et al., 1981. Some geochemical data on stylolites and heir host rocks. Eclog Geol Helv, 74: 217-224.

Sippel, R.P. and Glover, E.D., 1965. Structures in carbonate rocks made visible by by luminescence petrography. Science, 150; 1,283-1,287.

Stockdale, P.B., 1943. Stylolites: primary or secondary. Journal of Sedimentary Petrology, 13(1): 3-12.

Suppe, J., 1984. Introduction to Structural Geology. Prentice Hall.

Suppe, J., 1983. Geometry and kinematics of fault-bend folding. Am J Sci, 283(7): 684-721.

Tapp, B. and Wickham, J., 1987. Relationships of rock cleavage fabrics to incremental and accumulated strain in the Conococheague Formation, U.S.A., Journal of Structural Geology, ((4): 457-472.

Trurnit, P., 1968. Pressure solution phenomena in detrital rocks. Sedimentary Geology, 2: 89-114.

Weyl, P.K., 1958. The solution kinetics of calcite. Journal of Geology, 66: 163-176.

Weyl, P.K., 1959. Pressure solution and force of crystallization- a phenomenological theory. J Geophys Res, 64: 2001-2025.

Wones, D.R., ed., 1980. The Caledonides in the USA. VPI Department of Geological Sciences Memoir #2.

Woodward, N.B., ed., 1985. Valley and Ridge Belt: Balanced Structural sections, Pennsylvania to Alabama. University of Tennessee Dept. of Geological Science Studies in Geology 12.

Woodward, N.B., ed., 1989. Geometry and Deformation Fabrics in the Central and Southern Appalchian Valley and Ridge and Blue Ridge. AGU Field Trip Guidebook T 357.

Wojtal, S.F., 1989. Measuring displacement gradients and strains in faulted rocks. Journal of Structural Geology, 11(6): 669-678.

Wright, T.O. and Platt, L.B., 1982. Pressure dissolution and cleavage in the Martinsburg shale. American Journal of Science, 282: 122-135.